CONCEPTUAL ISSUES IN GEOMETRICALLY NONLINEAR ANALYSIS OF 3D FRAMED STRUCTURES

Bassam A. Izzuddin[1]

Key words: Framed Structures, Geometric Nonlinearity, Finite Rotations.

Abstract

This paper aims to clarify some of the conceptual issues which are related to the geometrically nonlinear analysis of 3D framed structures, and which have been a source of previous confusion. In particular, the paper discusses the symmetry of the tangent stiffness matrix and the nature of the element end moments. It is shown that a symmetric tangent stiffness matrix can always be achieved for a conservative system if the nodal equilibrium equations, including the equations which describe moment equilibrium, are identical to those derived from a variational energy approach. With regard to the element end moments, it is suggested that any definition can be adopted in formulating the geometrically nonlinear element response. Furthermore, it is proposed that any definition for nodal rotations expressing a unique vector transformation may be adopted without compromising modelling accuracy. The argument of this paper is validated with reference to three variants of a large displacement analysis method for 3D frames, where several illustrative examples are utilised.

[1] Reader in Computational Structural Mechanics, Dept. of Civil and Environmental Engineering, Imperial College, London SW7 2BU, U.K.

1 Introduction

The geometrically nonlinear analysis of 3D framed structures has received considerable attention by numerous researchers [1-9], particularly focussing on the treatment of the difficulties associated with finite nodal rotations in 3D space. These difficulties arise mainly from the non-commutativity of finite rotations about fixed axes and the dual issue of non-conservative moments about fixed axes. In order to model conservative structural frames, any applied moments must conform to a conservative definition (such as the quasi- or semi-tangential definitions), and the rotational freedoms must be associated with a definition which expresses a unique vector transformation (such as the semi-tangential definition) [2]. Depending on the nature of applied moments and the adopted definition for rotational freedoms, the two may be work conjugate (or 'corresponding' [2]), but that need not be the case.

The conventional approach to geometrically nonlinear analysis of 3D conservative frames has been to utilise an element tangent stiffness matrix which augments the constant stiffness matrix (used for linear analysis) with a geometric stiffness matrix proportional to the level of stresses within the element. In a pioneering contribution to the field, Argyris *et al.* [2] argued for expressing the nodal moment equilibrium equations using the semi-tangential definition of moments and for adopting the semi-tangential definition for the nodal rotational freedoms. They based their argument principally on the requirements that i) the element tangent stiffness matrix must be independent of the applied external loads, and that ii) the same transformation rules must be valid for both the constant and geometric stiffness matrices in order to account for arbitrary element orientations in 3D space. Furthermore, the adopted definitions for moments and rotations lead to a symmetric element tangent stiffness matrix, that is associated

with computational efficiency, and which is achieved by virtue of the fact that semi-tangential moments and rotations are work conjugate [2]. However, it should be noted that the first requirement is achieved only as long as the nodal moments applied to the structure are of the semi-tangential type (which of course includes zero moment loads), and that work conjugacy between the adopted definitions of moments and rotations is only valid up to a second order in rotations.

Several researchers adopted the semi-tangential definition for the element end moments in deriving the geometrically nonlinear element response [2,4,7]. Yang and Kuo [7] considered the buckling analysis of frames, where they used the governing differential equations for an element, in conjunction with nodal moment equilibrium in the deflected configuration, to obtain a symmetric tangent stiffness matrix. These authors insisted that, by using the 'conventional' definitions for bending moments and rotations, the internal bending moments should be interpreted as quasi-tangential moments. However, they indicated that the nodal moments behave as semi-tangential moments if the joint equilibrium conditions in the deformed state are enforced. Teh and Clarke [9], on the other hand, insisted that the internal moments are of the so-called 'fourth kind'. The same authors also suggested that the element tangent stiffness matrix is invariably asymmetric, without providing any qualification in respect of the type of applied moments and its conjugacy with the adopted definition for rotations.

This paper aims at clarifying the above issues, demonstrating that the symmetry of the tangent stiffness matrix is principally related to the work conjugacy of the adopted definition of moments used for the moment equilibrium equations and the adopted definition of rotational freedoms, and also illustrating that a symmetric tangent stiffness matrix is always possible to

achieve. It is also shown that a categorical classification of the element end moments is not required a priori, and that the geometrically nonlinear element response can be formulated, for any adopted definition of rotations which expresses a unique vector transformation, without making any assumptions in this respect.

It is emphasised that this paper is not principally concerned with assessing the accuracy of the previous methods discussed above, but instead focuses on conceptual issues raised in the development and presentation of such methods. For instance, while this paper shows that it is always possible to achieve a symmetric tangent stiffness matrix under certain *sufficient* formulation conditions, discussed in detail later, there is no implication that methods which employ an asymmetric tangent stiffness matrix are necessarily inaccurate. However, through demonstrating that the aforementioned *sufficient* and relatively relaxed conditions lead to a symmetric tangent stiffness matrix, it is contended that any suggestion of an inherent asymmetric property for the tangent stiffness matrix [9] is in fact erroneous. With regard to another conceptual issue, the paper suggests that any definition for the element end moments and the nodal rotational freedoms can be employed, although a definition implying work conjugacy of such entities is shown to have considerable computational advantages. Accordingly, there is no implication that methods employing specific definitions for the element end moments and nodal rotational freedoms are necessarily inaccurate. However, it is contended that the insistence on a single categorical classification for the element end moments [9] is also flawed.

Following a precise definition of the tangent stiffness matrix, the variational energy principle is utilised to demonstrate the aforementioned points. The relatively relaxed conditions under which the tangent stiffness matrix would be symmetric are highlighted, and the irrelevance of

an a priori assumption regarding the nature of element end moments is pointed out. These general conclusions are illustrated with reference to three variant approaches based on a method for large displacement analysis of 3D frames previously proposed by the author [8]. Several numerical examples are finally presented to demonstrate the relative accuracy of the three approaches, with the aim of validating the arguments made in this paper.

2 Definition of tangent stiffness matrix

By its very nature, nonlinear structural analysis is concerned with the satisfaction of a system of nonlinear equations, typically representing equilibrium conditions, through an iterative solution procedure. At any stage during such a procedure, there are errors in the equilibrium equations, representing out-of-balance forces/moments (**G**) between the applied load and the structural resistance, which can be expressed as:

$$\mathbf{G}_i = \mathbf{R}_i - \mathbf{P}_i^e \qquad (i = 1 \rightarrow n) \tag{1}$$

where, **R** represents the resistance forces/moments, $\mathbf{P}^e$ denotes the equivalent applied forces/moments in the same system (or adopting the same definition) as used for **R**, and n is the total number of translational/rotational freedoms.

An alternative approach could be to evaluate **G** using the same system/definition of the applied loading (**P**), in which case an equivalent resistance vector ($\mathbf{R}^e$) would be required:

$$\mathbf{G}_i = \mathbf{R}_i^e - \mathbf{P}_i \qquad (i = 1 \rightarrow n) \tag{2}$$

It is noted that $\mathbf{P}^e$ can be obtained from **P**, and similarly $\mathbf{R}^e$ can be determined from **R**, through distinct transformation processes which may depend on the values of nodal

displacements/rotations (**u**). However, these become identity transformations if all components of **P** already employ the same system/definition as the corresponding components in **R**, in which case the equilibrium equations in (1) and (2) become identical.

In the context of nonlinear structural analysis, the tangent stiffness matrix (**K**) is used to provide a first-order convergence guide towards zero **G**, and, therefore, a concise definition of **K** is:

$$\mathbf{K}_{i,j} = \frac{\partial \mathbf{G}_i}{\partial \mathbf{u}_j} \qquad (i, j = 1 \rightarrow n) \tag{3}$$

where, **u** is the vector of nodal freedoms.

3 Symmetry of tangent stiffness matrix

For a conservative structural system, the principle of stationary total potential energy (Π) can be used to establish the necessary equilibrium equations:

$$\frac{\partial \Pi}{\partial \mathbf{u}_i} = 0 \qquad (i = 1 \rightarrow n) \tag{4}$$

where Π is the sum of the system strain energy (U) and the load potential energy (–W):

$$\Pi = U - W \tag{5}$$

Combining the previous expressions, the equilibrium equations can be restated as:

$$\mathbf{R}_i - \mathbf{P}_i^e = 0 \qquad (i = 1 \rightarrow n) \tag{6}$$

in which,

$$\mathbf{R}_i = \frac{\partial U}{\partial \mathbf{u}_i} \tag{7}$$

$$\mathbf{P}_i^e = \frac{\partial W}{\partial \mathbf{u}_i} \tag{8}$$

Whereas W is a function of the applied loading (**P**) and the nodal freedoms (**u**), U is only dependent on **u**. If **P** is work conjugate with **u**, that is:

$$W = \sum_{i=1}^{n} \mathbf{P}_i \, \mathbf{u}_i \tag{9}$$

then $\mathbf{P}^e$ would be identical to **P**, but otherwise $\mathbf{P}^e$ would be a transformation of **P** which may be dependent on **u**.

It is noted that the above nonlinear equilibrium conditions (6-8) are normally obtained, in an identical form, using the virtual work method, where the virtual displacement modes are those associated with infinitesimal changes of individual freedoms $\mathbf{u}_i$. However, the principle of stationary total potential energy is utilised here simply to facilitate the exposition of conceptual issues which have been a source of previous confusion.

Observing the equilibrium conditions (6-8), it is now clear that the first expression for **G** in (1) can be thought of as representing the out-of-balance between **R** and $\mathbf{P}^e$ which are work conjugate with **u**. If such a definition is adopted for **G**, the tangent stiffness matrix defined in (3) can be expressed as:

$$\mathbf{K}_{i,j} = \frac{\partial \mathbf{R}_i}{\partial \mathbf{u}_j} - \frac{\partial \mathbf{P}_i^e}{\partial \mathbf{u}_j} = \frac{\partial^2 \Pi}{\partial \mathbf{u}_i \, \partial \mathbf{u}_j} \qquad (i, j = 1 \rightarrow n) \tag{10}$$

From this expression, it is obvious that **K** becomes symmetric for a conservative system which possesses a continuous total potential energy (Π) that is uniquely defined by the adopted freedoms (**u**), if the work conjugate equilibrium equations are employed. Furthermore, the expression of **K** in (10) simplifies to:

$$\mathbf{K}_{i,j} = \frac{\partial \mathbf{R}_i}{\partial \mathbf{u}_j} = \frac{\partial^2 U}{\partial \mathbf{u}_i \, \partial \mathbf{u}_j} \qquad (i, j = 1 \rightarrow n) \tag{11}$$

if either **P** is work conjugate with **u** or $\mathbf{P}^e$ is independent of **u**, in which case **K** becomes independent of **P**. Of course, the same simplification is achieved if the possible components of **P** which violate the work conjugacy with **u** are all associated with zero values.

In view of the above, it is evident that **K** could be asymmetric only if the work conjugate equilibrium equations in (1) are not adopted to the preference of some other form, such as that given by (2). However, it is noted again that this particular form becomes identical to (1), thus leading to a symmetric **K**, if the applied load **P** is work conjugate with **u**.

The above conclusions can be re-stated more specifically with reference to the geometrically nonlinear analysis of 3D elastic frames. Typically for structural models of such frames, each node would be associated with 3 translational and 3 rotational freedoms, and the corresponding applied nodal loads consist of 3 forces and 3 moments. Since it is always possible to define the applied nodal forces in a manner which achieves work conjugacy with the translational freedoms, the principle source of difficulty therefore arises from the variety of ways for generating conservative nodal moments and the possibility that the applied moments may not be work conjugate with the adopted definition of rotational freedoms. However, as shown above, it is possible even in such a case to achieve a symmetric **K** if the

work conjugate equilibrium equations are employed, although **K** could consequently become dependent on the applied moments. Nevertheless, given that most framed structures are not subject to directly applied moments, and that most conservative moments can in any case be represented by forces acting at the ends of additional rigid link elements, the need to transform applied moments and the dependency of the symmetric **K** on the applied loading can be circumvented, as effected in the method proposed previously by the author [8].

4 Nature of element end moments

There has been a considerable measure of confusion in some previous research works surrounding the nature of element end moments, which this Section aims to address. This confusion stems mainly from attempts to classify the nature of internal bending and torsional moments of beam-column elements, as these moments were deemed, inappropriately, to have the same behavioural characteristics of the element nodal moments. Yang and McGuire [4] observed that internal bending and torsional moments appear to be of the quasi-tangential and semi-tangential types, respectively, although they noted the inconsistency of adopting different definitions for the 'related' element nodal moments, particularly in modelling a structure with non-collinear members. Accordingly, they opted for a uniform semi-tangential moment definition for the three components of nodal moment, but they noted that this issue required further research. More recently, Teh and Clarke [9] rejected the semi-tangential definition for nodal moments adopted by Argyris *et al.* [2] and by Yang and McGuire [4], and they insisted that element end moments are in fact of the so-called 'fourth kind'.

Evidently, the main cause behind the above confusion is the inappropriate and unnecessary linkage on the element level between the behavioural property of internal moments and that of

end nodal moments. This linkage is incorrect, since internal bending and torsional moments are generalised stress entities which perform work over generalised curvature and twist strains, thus providing a measure of the stored strain energy over an infinitesimal element length. Element end moments, on the other hand, are nodal entities which perform work over nodal rotations, thus providing a measure of the element contribution to the resistance against applied nodal moments (often evaluated in a 'weak' finite element sense). Therefore, classifications such as semi-tangential and quasi-tangential are only appropriate in the context of element end moments, since only in this context the influence of finite nodal rotations on the form of the rotational work expression becomes relevant. Emphasising this point further, it is entirely possible to derive the large displacement nodal response of beam-column elements without reference to the concept of internal bending and torsional moments, but instead utilising expressions for the strain energy which are based directly on the material stresses and strains. This is illustrated clearly by considering the two distinct elements of Fig. 1 which have an identical 'nodal' interface at the ends, where the first element employs a uniform solid circular cross-section, whereas the second element utilises six internal axial struts. It is evident that the concept of internal bending and torsional moments is only useful for formulating the nodal response of the first element and not that of the second element. On the other hand, the large displacement nodal response of both elements can be formulated, without any undue compromise of accuracy, by starting from expressions for the element strain energy which are based directly on material stresses and strains.

Having established that classification should not be applied to internal bending and twisting moments but only to end nodal moments, it is further suggested that any definition for the element end moments can be adopted, again without compromising accuracy. It would be

convenient from a computational perspective, however, that the adopted definition enables the moment equilibrium at a particular node to be derived from an overall moment resistance which is a simple summation of the various element contributions. In view of this, it is proposed that the adopted definition for nodal moments should simply be one which implies work conjugacy with the adopted definition for nodal rotations. This of course would have the added benefit of leading to a symmetric tangent stiffness matrix, as discussed in Section 3. It should also be emphasised that any definition for nodal rotations which expresses a unique vector transformation can be employed. In addition to the semi-tangential definition adopted by Argyris *et al.* [2], it is entirely valid to use other definitions for nodal rotations, such as a definition based on modified Euler angles [10], although the corresponding work conjugate moments in this case would differ from the semi-tangential type.

Finally, it is suggested that the terms ‘bending’ and ‘torsional’ moments should be reserved for internal generalised stresses which are work conjugate with generalised curvatures and twisting strains on the cross-sectional level, and that the application of these terms to nodal resistance moments at the element ends should be avoided.

5 Variant methods for large displacement analysis of 3D frames

The above discussion is illustrated here with reference to three variant approaches based on a large displacement analysis method for 3D frames, which was previously proposed by the author [8]. This method is identically derived from the variational energy principle, outlined earlier in this paper, or from the equivalent method of virtual work, and it accounts for the effects of large nodal displacements and rotations but for small strains within the component elements. The nodal displacements and rotations describe compatible deformation modes over

the structure, which present an approximation of the exact structural deflected shape. Accordingly, equilibrium is satisfied in a weak discrete sense over the available modes, although the level of approximation is guaranteed to improve with the inclusion of more deformation modes through additional nodes.

In formulating the large displacement response of a beam-column element, the proposed method distinguishes between the global reference system, where deformation compatibility and nodal equilibrium of the overall structure are enforced, and a local reference system, which is an element-specific system used for quantifying the element strain energy.

In the global reference system, twelve nodal freedoms are utilised for an element:

$$ {}_{g}\mathbf{u} = \left\langle u_1, v_1, w_1, \alpha_1, \beta_1, \gamma_1, u_2, v_2, w_2, \alpha_2, \beta_2, \gamma_2 \right\rangle^{T} \tag{12} $$

as illustrated in Fig. 2. Consideration is given in the variant approaches to two alternative descriptions of global nodal freedoms, namely incremental (in relation to the previous equilibrium configuration) or total (in relation to the initial undeformed configuration), as elaborated in the following sub-sections.

The global nodal displacements define the orientation of the element chord (${}_{x}\mathbf{c}$) in the current iterative configuration, whereas the global nodal rotations (α, β, γ) define a unique vector transformation matrix (${}_{r}\mathbf{T}$). Two alternative definitions of global rotations are considered in the variant approaches: the first is based on a resultant rotation vector [8], whereas the second employs modified Euler angles [10]; accordingly, ${}_{r}\mathbf{T}$ is dependent on the variant approach as detailed later. The rotational transformation matrices at the two element nodes determine the current cross-sectional orientation vectors (Fig. 2):

$$\left.\begin{aligned} {}^{1}_{y}\mathbf{c}_i &= \sum_{j=1}^{3}\left({}^{1}_{r}\mathbf{T}_{i,j}\ {}^{1}_{y}\mathbf{c}^{o}_{j}\right); \quad {}^{1}_{z}\mathbf{c}_i = \sum_{j=1}^{3}\left({}^{1}_{r}\mathbf{T}_{i,j}\ {}^{1}_{z}\mathbf{c}^{o}_{j}\right) \\ {}^{2}_{y}\mathbf{c}_i &= \sum_{j=1}^{3}\left({}^{2}_{r}\mathbf{T}_{i,j}\ {}^{2}_{y}\mathbf{c}^{o}_{j}\right); \quad {}^{2}_{z}\mathbf{c}_i = \sum_{j=1}^{3}\left({}^{2}_{r}\mathbf{T}_{i,j}\ {}^{2}_{z}\mathbf{c}^{o}_{j}\right) \\ {}^{21}_{y}\mathbf{c}_i &= \sum_{j=1}^{3}\left({}^{2}_{r}\mathbf{T}_{i,j}\ {}^{1}_{y}\mathbf{c}^{o}_{j}\right) \end{aligned}\right\} \tag{13}$$

in which,

$$\left.\begin{aligned} {}^{1}_{r}\mathbf{T} &= {}_{r}\mathbf{T}(\alpha_1,\beta_1,\gamma_1) \\ {}^{2}_{r}\mathbf{T} &= {}_{r}\mathbf{T}(\alpha_2,\beta_2,\gamma_2) \end{aligned}\right\} \tag{14}$$

where ${}^{1}_{y}\mathbf{c}^{o}$, ${}^{1}_{z}\mathbf{c}^{o}$, ${}^{2}_{y}\mathbf{c}^{o}$ and ${}^{2}_{z}\mathbf{c}^{o}$ represent the cross-sectional orientation vectors either in the previous equilibrium configuration or in the initial undeformed configuration, depending on the variant approach. Note that ${}^{21}_{y}\mathbf{c}$ in (13) is a fictitious vector used for the evaluation of the element twist rotation [8], as demonstrated later.

The element strain energy is quantified with reference to a local system, which coincides with the element chord in the current iterative configuration, as depicted in Fig. 2, and which isolates the strain inducing modes from stress free rigid body modes. This local convected system has been termed an Eulerian system [8,11], based on a close analogy with reference systems used for problems of fluid mechanics, although a distinctive and more recent term is also a co-rotational system [12]. In the local system, six basic degrees of freedom are employed (Fig. 2):

$${}_{c}\mathbf{u} = \left\langle \theta_{1y}, \theta_{1z}, \theta_{2y}, \theta_{2z}, \Delta, \theta_{T} \right\rangle^{T} \tag{15}$$

which provide an intermediate step for determining the element strains corresponding to a set of global displacements and rotations (${}_{g}\mathbf{u}$).

For practical small strain problems, the local deformations (${}_{c}\mathbf{u}$) can be assumed to be small, with this assumption becoming increasingly justified as more elements are used per member [13]. The global nodal displacements combined with ${}^{1}_{y}\mathbf{c}$, ${}^{1}_{z}\mathbf{c}$, ${}^{2}_{y}\mathbf{c}$, ${}^{2}_{z}\mathbf{c}$ and ${}_{x}\mathbf{c}$ in the current iterative configuration determine the local deformations ${}_{c}\mathbf{u}$, thus defining an implicit nonlinear relationship between the local and global freedoms:

$$ {}_{c}\mathbf{u} = \psi({}_{g}\mathbf{u}) \tag{16} $$

the details of which depend on the particular variant approach, as discussed in the following sub-sections.

In the local system, approximation shape functions are used to relate the element deformed shape to ${}_{c}\mathbf{u}$, thus enabling the quantification of the element strain energy (U^{e}) in terms of ${}_{c}\mathbf{u}$. The variation of the U^{e} with ${}_{c}\mathbf{u}$ defines the work conjugate local resistance forces/moments of the element:

$$ {}_{c}\mathbf{f}_{m} = \frac{\partial U^{e}}{\partial {}_{c}\mathbf{u}_{m}} \quad (m = 1 \rightarrow 6) \tag{17} $$

where,

$$ {}_{c}\mathbf{f} = \left\langle M_{1y}, M_{1z}, M_{2y}, M_{2z}, F, M_{T} \right\rangle^{T} \tag{18} $$

The determination of ${}_c\mathbf{f}$ from ${}_c\mathbf{u}$, in view of the assumption that the latter is small, can be established using a linear local formulation, as detailed in Appendix A.1, although a geometrically nonlinear formulation for the local response enables a certain level of accuracy to be achieved with fewer elements per member. One such nonlinear formulation for the local response is provided by a quartic element [14], which is intended to model the beam-column effect in the local system using only one element per member. The quartic beam-column element is derived and verified elsewhere [14], but is utilised in the subsequent examples of this paper to illustrate the relative accuracy of the three considered variant approaches for the geometrically nonlinear analysis of space frames. Given that the quartic element can be utilised with the three approaches without any modification to its local response characteristics, this paper will focus only on the transformation of the local element response to its global response, as influenced by the variant approaches.

It is notable that five components of ${}_c\mathbf{f}$ are in fact moments, the classification of which in relation to the local rotations in ${}_c\mathbf{u}$ is not very important, since these rotations are assumed to be small. However, the classification of these five moments in relation to global rotations would show that they are moments of the follower type. Given that the considered variant approaches require the global element end moments to be work conjugate with the adopted definition of nodal rotations, a transformation would be necessary to obtain the global end moments from the local end moments. Such a transformation is indirectly effected in the following expression, which employs chain differentiation rules, for the work conjugate global resistance forces/moments in terms of ${}_c\mathbf{f}$:

$$ {}_{g}\mathbf{f}_{i} = \frac{\partial U^{e}}{\partial_{g}\mathbf{u}_{i}} = \sum_{m=1}^{6}\left(\frac{\partial_{c}\mathbf{u}_{m}}{\partial_{g}\mathbf{u}_{i}} \frac{\partial U^{e}}{\partial_{c}\mathbf{u}_{m}} \right) = \sum_{m=1}^{6}\left(\mathbf{T}_{i,m}\ {}_{c}\mathbf{f}_{m} \right) \quad (i = 1 \rightarrow 12) \tag{19} $$

where **T** is a 12×6 transformation matrix dependent on the specific variant approach, as detailed in Appendix A.2.

Since most conservative moments can be simulated by means of conservative forces applied at the ends of additional rigid link elements, it is assumed that no moments are applied directly at the nodes, thus achieving a simplification in the equilibrium equations, as discussed in Section 3. This further simplifies the expression for the tangent stiffness matrix, which becomes independent of the applied loading:

$$ {}_{g}\mathbf{k}_{i,j} = \frac{\partial_{g}\mathbf{f}_{i}}{\partial_{g}\mathbf{u}_{j}} = \frac{\partial^{2} U^{e}}{\partial_{g}\mathbf{u}_{i}\,\partial_{g}\mathbf{u}_{j}} = \sum_{m=1}^{6}\sum_{n=1}^{6}\left(\mathbf{T}_{i,m}\ {}_{c}\mathbf{k}_{m,n}\ \mathbf{T}_{i,n} \right) + \sum_{m=1}^{6}\left(\mathbf{g}_{i,j,m}\ {}_{c}\mathbf{f}_{m} \right) \quad (i, j = 1 \rightarrow 12) \tag{20} $$

where,

$$ {}_{c}\mathbf{k}_{m,n} = \frac{\partial_{c}\mathbf{f}_{m}}{\partial_{c}\mathbf{u}_{n}} = \frac{\partial^{2} U^{e}}{\partial_{c}\mathbf{u}_{m}\,\partial_{c}\mathbf{u}_{n}} \qquad (m, n = 1 \rightarrow 6) \tag{21} $$

$$ \mathbf{g}_{i,j,m} = \frac{\partial \mathbf{T}_{i,m}}{\partial_{g}\mathbf{u}_{j}} = \frac{\partial^{2}\,{}_{c}\mathbf{u}_{m}}{\partial_{g}\mathbf{u}_{i}\,\partial_{g}\mathbf{u}_{j}} \qquad (i, j = 1 \rightarrow 12\ ; \quad m = 1 \rightarrow 6) \tag{22} $$

In the above expressions, ${}_{c}\mathbf{k}$ is a 6×6 local tangent stiffness matrix, presented in Appendix A.1 for a linear local formulation and derived elsewhere for the quartic element [14], whilst **g** is a 12×12×6 array determining the geometric stiffness matrix and dependent on the specific variant approach, as detailed in Appendix A.3. It is of course worth noting that the global element tangent stiffness matrix in (20) is always symmetric, regardless of the specific details

of the variant approach, as would be expected, since the adopted equilibrium equations correspond to forces and moments which are work conjugate with the adopted definition for the global degrees of freedom.

Hereafter, the three variant approaches are discussed in detail, the only variants being i) whether the global freedoms are total or incremental, and ii) whether the global rotations follow a resultant vector definition [8] or a modified Euler definition [10]. As mentioned previously, these variants have implications on the rotational transformation matrix (${}_{r}\mathbf{T}$), the implicit relationship between the local and global freedoms (ψ), the force transformation matrix (**T**), and the geometric stiffness matrix as determined by **g**.

5.1 Variant method (A): incremental with resultant vector rotations

This is the original method proposed by the author [8], where an incremental description is adopted for the global element freedoms (${}_{g}\mathbf{u}$), and the local deformations (${}_{c}\mathbf{u}$) are evaluated incrementally, in both instances with reference to last known equilibrium configuration. The adopted definition for rotations is based on a resultant rotational vector, the effect of which is approximated by a second-order transformation matrix [8]:

$$ {}_{r}\mathbf{T}(\alpha,\beta,\gamma) = \begin{bmatrix} 1-\frac{\beta^2+\gamma^2}{2} & -\gamma+\frac{\alpha\,\beta}{2} & \beta+\frac{\alpha\,\gamma}{2} \\ \gamma+\frac{\alpha\,\beta}{2} & 1-\frac{\alpha^2+\gamma^2}{2} & -\alpha+\frac{\beta\,\gamma}{2} \\ -\beta+\frac{\alpha\,\gamma}{2} & \alpha+\frac{\beta\,\gamma}{2} & 1-\frac{\alpha^2+\beta^2}{2} \end{bmatrix} \qquad (23) $$

Given the incremental nature of ${}_{g}\mathbf{u}$, such an approximation is reasonable for most practical applications, with any errors reducing as the number of increments is increased. It is noted that at least a second-order expression for ${}_{r}\mathbf{T}$ is essential in the context of geometrically nonlinear analysis. Furthermore, it can be shown that the adopted definition for nodal rotations approximates the semi-tangential definition [2] to a second order. Consequently, the nature of global nodal moments which are work conjugate with the adopted definition for rotations is of the semi-tangential type [8], only that it should be considered in an incremental context due to the incremental nature of the considered rotations. However, given that any conservative moments are to be represented by forces applied to the ends of additional rigid link elements, a classification for the work conjugate moments is not necessary and is in fact purely of academic interest.

In this variant method, the orientation vectors (${}^{1}_{y}\mathbf{c}^{o}$, ${}^{1}_{z}\mathbf{c}^{o}$, ${}^{2}_{y}\mathbf{c}^{o}$, ${}^{2}_{z}\mathbf{c}^{o}$) correspond to the previous equilibrium configuration and are always orthogonal to the previous chord vector (${}_{x}\mathbf{c}^{o}$). The global nodal displacements and the current orientation vectors, established from (13), (14) and (23), determine the increment of the local deformations ($\delta_{c}\mathbf{u}$) according to:

$$\left.\begin{aligned} X_E = X_E^o + u_2 - u_1;\;\; Y_E = Y_E^o + v_2 - v_1;\;\; Z_E = Z_E^o + w_2 - w_1 \\ L_E = \sqrt{{X_E}^2 + {Y_E}^2 + {Z_E}^2} \end{aligned}\right) \qquad (24.a)$$

$${}_{x}\mathbf{c} = \left\langle \frac{X_E}{L_E}, \frac{Y_E}{L_E}, \frac{Z_E}{L_E} \right\rangle^{T} \qquad (24.b)$$

$$\left.\begin{aligned}
\delta\theta_{1y} &= -\sum_{i=1}^{3}\left({}_{x}\mathbf{c}_i \;\; {}^{1}_{y}\mathbf{c}_i\right) \\
\delta\theta_{1z} &= -\sum_{i=1}^{3}\left({}_{x}\mathbf{c}_i \;\; {}^{1}_{z}\mathbf{c}_i\right) \\
\delta\theta_{2y} &= -\sum_{i=1}^{3}\left({}_{x}\mathbf{c}_i \;\; {}^{2}_{y}\mathbf{c}_i\right) \\
\delta\theta_{2z} &= -\sum_{i=1}^{3}\left({}_{x}\mathbf{c}_i \;\; {}^{2}_{z}\mathbf{c}_i\right) \\
\delta\Delta &= L_E - L_E^o \\
\delta\theta_T &= \sum_{i=1}^{3}\left({}^{1}_{z}\mathbf{c}_i \;\; {}^{21}_{y}\mathbf{c}_i\right)
\end{aligned}\right\} \qquad (24.c)$$

where X_E, Y_E and Z_E are the element projections on the three respective global axes, with the (o) right superscript for all entities indicating values in the previous equilibrium configuration.

The local deformations are obtained incrementally:

$$ {}_{c}\mathbf{u} = {}_{c}\mathbf{u}^{o} + \delta_{c}\mathbf{u} \qquad (25)$$

thus defining the implicit relationship, expressed by (16), between the local and global element freedoms. The accuracy of the incremental evaluation of ${}_{c}\mathbf{u}$ improves with the number of incremental steps, although any errors are negligible for most practical applications, where the rotational components of ${}_{c}\mathbf{u}$ would be small due to the assumption of small strains.

With ${}_{c}\mathbf{u}$ corresponding to ${}_{g}\mathbf{u}$ established, the local element forces/moments (${}_{c}\mathbf{f}$) and tangent stiffness matrix (${}_{c}\mathbf{k}$) are determined according to the element formulation, such as given for the quartic beam-column element [14]. These are transformed to global element

forces/moments (${}_{g}\mathbf{f}$) and tangent stiffness matrix (${}_{g}\mathbf{k}$) using (19) and (20), where **T** and **g** are determined, respectively, as the first and second partial derivatives of ${}_{c}\mathbf{u}$ with respect to ${}_{g}\mathbf{u}$, as detailed in Appendices A.2 and A.3.

It should be noted that, after equilibrium is achieved for the current incremental step, the orientation vectors (${}^{1}_{y}\mathbf{c}$, ${}^{1}_{z}\mathbf{c}$, ${}^{2}_{y}\mathbf{c}$, ${}^{2}_{z}\mathbf{c}$) are always re-normalised to an orthogonal position relative to ${}_{x}\mathbf{c}$ [8] so that the above expressions for ${}_{c}\mathbf{u}$ can be applied for the subsequent incremental step.

5.2 Variant method (B): incremental with modified Euler angles

In order to consider the validity of alternative definitions of rotation, this method adopts the modified Euler definition [10] for the global nodal rotations, with all other aspects identical to variant method (A). The adopted definition corresponds to successive rotations about follower axes, where the rotations are applied in the order (γ, β, α), thus leading to the following vector transformation matrix:

$$ {}_{r}\mathbf{T}(\alpha,\beta,\gamma) = \begin{bmatrix} c_\gamma\, c_\beta & -s_\gamma\, c_\alpha + c_\gamma\, s_\beta\, s_\alpha & s_\gamma\, s_\alpha + c_\gamma\, s_\beta\, c_\alpha \\ s_\gamma\, c_\beta & c_\gamma\, c_\alpha + s_\gamma\, s_\beta\, s_\alpha & -c_\gamma\, s_\alpha + s_\gamma\, s_\beta\, c_\alpha \\ -s_\beta & c_\beta\, s_\alpha & c_\beta\, c_\alpha \end{bmatrix} \qquad (26.a) $$

in which,

$$ c_a = \cos(a); \quad s_a = \sin(a) \qquad (26.b) $$

It is again interesting to classify the moments which are work conjugate with the above definition of rotations, although such a classification is not necessary when applied moments

are represented by forces acting at the ends of additional rigid link elements. By determining the infinitesimal rotations about fixed axes which are equivalent to infinitesimal increments in the adopted rotations (α, β, γ) [8], it is possible to transform the work conjugate moments to moments about fixed axes, as given by:

$$\begin{Bmatrix} M_x^f \\ M_y^f \\ M_z^f \end{Bmatrix} = \begin{bmatrix} c_\gamma / c_\beta & -s_\gamma & c_\gamma s_\beta / c_\beta \\ s_\gamma / c_\beta & c_\gamma & s_\gamma s_\beta / c_\beta \\ 0 & 0 & 1 \end{bmatrix} \begin{Bmatrix} M_x \\ M_y \\ M_z \end{Bmatrix} \tag{27}$$

It can be shown from (27) that each of M_x, M_y and M_z specifies a moment value about its respective 'transformed' axis with zero moment projections on the other two 'transformed' axes. The 'transformed' axes are defined as follows: X is rotated by γ followed by β, Y is rotated by γ, and Z is fixed.

As with method (A), the global elements freedoms in this variant method are incremental; however, unlike method (A), the rotation matrix ($_r\mathbf{T}$) here is exact, and hence there is no approximation in determining the element orientation vectors that can be influenced by the number of incremental steps. Nevertheless, the local element deformations ($_c\mathbf{u}$) are still evaluated incrementally, and hence the number of steps could have some influence on accuracy, although, with $_c\mathbf{u}$ being small for most practical applications, such an influence would be of minor significance.

5.3 Variant method (C): total with modified Euler angles

Following on from the above discussion, the question arises whether accuracy of the adopted nonlinear analysis method is compromised if a total, instead of an incremental, formulation is

employed, which might in turn compromise the general argument of this paper. Accordingly, this variant method considers a total formulation in which all prior entities, denoted in the above expressions by the (o) right superscript, refer to the initial undeformed configuration. In order to remove the approximation associated with the rotational transformation matrix, the modified Euler definition of (26) is adopted. This leaves only the approximation associated with the evaluation of the local element deformations (${}_c\mathbf{u}$) from (24) and (25), ${}_c\mathbf{u}^o$ being zero as referred to the initial configuration, where an identity is assumed between an angle and its sine. However, it is again noted that this approximation is adequate for small ${}_c\mathbf{u}$, which is the case in most practical applications; furthermore, given that ${}_c\mathbf{u}$ can be reduced steadily through increasing the number of elements per member [13], any errors arising from this approximation should diminish considerably through mesh refinement.

6 Examples

The discussion presented in this paper is supported herein by means of several examples illustrating the relative accuracy of variant methods (A) to (C), each of these methods representing a particular instantiation of the general variational energy or virtual work principles. While method (A) was verified extensively in previous work [8,14-16], particular consideration is given here to i) large displacement problems which involve finite rotations in 3D space as well as applied moments, ii) the influence of an alternative definition of rotations as in method (B), and iii) the influence of a total formulation for the large displacement response as in method (C). All presented examples utilise the quartic beam-column element [14], which is implemented in the nonlinear structural analysis program ADAPTIC v2.9.6 [15], and which can be employed, without modification, with any of the three considered

variant methods. It is worth noting that in all examples where moment loads are applied, the moments are represented by means of conservative forces applied at the end of additional rigid link elements instead of being directly applied as nodal moment loads, as required by the three variant methods.

6.1 Cantilever subject to end moment

A cantilever is considered under the action of two forms of quasi-tangential moment as well as a semi-tangential moment applied at its tip, as illustrated in Fig. 3. The buckling response of this cantilever was considered previously by Argyris *et al.* [2], where the following buckling moments were predicted with 10 elements:

$$M_{cr}^{QT1} = M_{cr}^{QT2} = 3.93103 \text{ N.cm}, \quad M_{cr}^{ST} = 7.88632 \text{ N.cm} \tag{21}$$

The nonlinear response of the cantilever is determined first using variant method (A) with three alternative meshes of 2, 4 and 8 quartic elements, where the moments are modelled by means of in-plane forces applied to the ends of rigid link elements. In addition, very small out-of-plane forces are applied in order to initiate lateral buckling. The results depicted in Fig. 4 show that very good accuracy is achieved in comparison with the previous buckling predictions [2]. It is worth noting that for the quasi-tangential moments, 2 quartic elements provide adequate accuracy, and that although the buckling moments are identical for the two quasi-tangential forms, the post-buckling behaviour is markedly different. This is attributed to the different buckling modes, as can be observed from the final deflected shapes in Fig. 5. For the semi-tangential moment, 4 quartic elements are required for comparable accuracy to the quasi-tangential cases (Fig. 4). This is again attributed to the different buckling mode which

places a greater demand on the approximation of the twist rotation along the cantilever length, as illustrated in the final deflected shape of Fig. 5.

The relative performance of variant methods (A) to (C) is illustrated in Fig. 6, where all the results are based on a mesh of 8 quartic elements. It is notable that methods (A) and (B) provide identical results for the three types of applied moment, thus confirming that alternative definitions for rotations may be adopted without necessarily compromising solution accuracy. This also confirms the adequacy of the simplified second-order rotation matrix of the original method (A) within an incremental approach [8], the number of increments used for this problem being 40 (Fig. 6). The depicted results also demonstrate the accuracy of the total formulation approach of method (C), where almost identical results are achieved in comparison with the two other incremental variant methods. An interesting feature of method (C) is that its accuracy is independent of the number of incremental steps, but is in fact determined by the number of elements used which controls the magnitude of local deformations [13]. Therefore, any inaccuracies, such as the slight discrepancy at large displacements for the case of the semi-tangential moment (Fig. 6), can be addressed through mesh refinement. This point is illustrated clearly in the last space dome example.

6.2 L-frame subject to end force

The L-frame, shown in Fig. 7, is subjected to an end force P, where load application in both the positive and negative x-directions is considered, referred to as P+ and P– , respectively. The buckling forces for this frame were also obtained by Argyris *et al.* [2], where the following values were reported using 10 elements:

$$P_{cr}^{+} = 1.50148 \text{ N}, \quad P_{cr}^{-} = 0.918391 \text{ N} \tag{22}$$

The nonlinear response of the frame is obtained first using method (A) with 1, 2 and 4 quartic elements per member, again assuming a very small out-of-plane end force in order to initiate lateral buckling, where the results in Fig. 8 show good agreement against the previous buckling predictions [2]. As with the previous example, the number of elements required for adequate approximation depends on the complexity of the buckling mode, where case P+ is associated with a relatively more complex mode than for case P–, thus requiring more elements for equivalent accuracy. The final deflected shapes for both cases P+ and P– are illustrated in Fig. 9, which reflect the different buckling modes under the two loading cases.

The relative performance of variant methods (A) to (C) is depicted in Fig. 10, where the results are obtained using a mesh of 4 quartic elements per member. Evidently, the same conclusions reached in the previous example, relating to the accuracy of the three variant methods, apply here as well.

6.3 L-frame subject to end moment

The same L-frame of the previous example, but with the member cross-sectional properties of the first cantilever example, is considered here under the action of two forms of quasi-tangential moment as well as a semi-tangential moment, as illustrated in Fig. 11. Again, the buckling characteristics of this system were investigated by Argyris *et al.* [2], where the following buckling moments were predicted with 10 elements:

$$M_{cr}^{QT1} = 0.493489 \text{ N.cm}, \quad M_{cr}^{QT2} = 3.43658 \text{ N.cm}, \quad M_{cr}^{ST} = 0.986979 \text{ N.cm} \tag{23}$$

The nonlinear response of the frame is obtained first using method (A) with 1, 2 and 4 quartic elements per member, assuming very small out-of-plane forces, where the results are shown in Fig. 12. Comparison of the depicted results against the previously predicted buckling moments [2] shows good agreement, except that the results for the two cases of quasi-tangential moment appear to be transposed. Given that the variant methods proposed here are not sensitive to the type of applied moment, as this is modelled by means of forces applied to rigid link elements, it is suggested that, in the absence of a more basic problem with the allowance of Argyris *et al.* [2] for quasi-tangential moments within their geometric stiffness matrix, these authors might have inadvertently transposed the results. As with the previous example, more elements are required for adequate approximation of the QT1 buckling response than for the other two moment types, with it being associated with a more demanding buckling mode. While 1 element per member provides excellent accuracy for the QT2 and ST cases, at least 2 elements per member are required to achieve a similar level of accuracy for the QT1 case.

It is also worth noting that the ST buckling moment is very close to twice that of the lower QT buckling moment (i.e. QT2). This can be explained by the fact that the ST moment consists of half the aggregate of the two QT moments, and hence buckling in the much lower QT2 mode would be initiated when the ST moment is approximately twice the corresponding QT buckling moment. This is confirmed by observing the final deflected shapes in Fig. 13, where it is evident that the QT2 and ST modes are almost identical.

The relative performance of variant methods (A) to (C) is depicted in Fig. 14, where a mesh of 4 quartic elements per member is employed. Again, the same conclusions reached in the first example, relating to the accuracy of the three variant methods, apply to this example.

6.4 Space dome subject to vertical apex load

The space dome structure, shown in Fig. 15, has been widely considered in the verification of nonlinear analysis methods for 3D frames. In previous work of the author [8], the load deflection response of the dome was established using 1 quartic element per member. Recently, Teh and Clarke [9] considered the same problem, and they alluded to the point that the analysis methods proposed by several other researchers, including the author's original method [8], did not seem to be able to predict the lowest buckling mode of the dome. They attributed the success of their method in detecting such a mode to the incorporation of an asymmetric geometric stiffness matrix, claiming that the tangent stiffness matrix for large displacement analysis of space frames is invariably asymmetric.

The aim here is therefore to show that the author's original method [8], that is method (A), is intrinsically capable of predicting the lowest buckling mode of the dome, but that due to the assumption of a perfect dome geometry such a mode was not initiated in the previous simulation, and only the fundamental equilibrium path was traced [8]. Accordingly, it is aimed to show that the adoption of a symmetric tangent stiffness matrix has no related shortcomings, thus adding further weight to the argument of this paper that it is always possible to formulate and utilise a symmetric tangent stiffness matrix for geometrically nonlinear structural analysis without compromising accuracy.

In order to illustrate the accuracy of methods based on the variational energy principle, which as demonstrated in this paper enable the use of a symmetric tangent stiffness matrix, the nonlinear analysis is performed first with the original method (A) on perfect and imperfect dome configurations. For the imperfect dome, small random perturbations are introduced to

the nodal positions, which vary between 1mm and 3mm, thus enabling a close approximation of the secondary equilibrium path without the need for a bifurcation detection technique. Such a technique would simply enable the detection of a bifurcation point along the current equilibrium path, in most cases due to a perfect structural and loading configuration, and it could be used to guide the nonlinear analysis method along one of the bifurcating paths. However, it must be emphasised that such a technique would have no influence over the accuracy of the analysis method in approximating a specific equilibrium path, and it certainly would have no implications regarding the conceptual issues addressed in this paper.

The nonlinear analysis is undertaken with method (A) using 1 and 2 quartic elements per member, where the predicted responses are shown in Fig. 16. These results illustrate the ability of this original method to predict the lowest buckling mode and to trace the associated post-buckling path when an imperfect dome is considered. It should be noted, that the obtained results compare favourably against the predictions of Teh and Clarke [9], both in the pre-buckling and post-buckling ranges. Significantly, the proposed method is also able to provide an excellent prediction with only 1 element per member, for both the perfect and imperfect domes.

To emphasise the distinct modes involved in this simulation, the final deflected shapes of the perfect and imperfect domes are depicted in Fig. 17, both in plan and perspective views. It is evident that the introduction of small imperfections activates the lowest buckling mode, which involves a planar rotational mode. In the absence of such imperfections, the dome deflects in a mode which is fully symmetric about the dome apex in plan view.

In view of the above, it is contended that the symmetry of the tangent stiffness matrix is not a shortcoming of the previously proposed method [8]. To the contrary, the ability of this

method to predict the geometrically nonlinear response using a computationally efficient tangent stiffness matrix, by virtue of its symmetry, is considered to be an important advantage.

The results in Fig. 18 demonstrate that the above conclusion applies also to variant methods (B) and (C), both of which utilise a symmetric tangent stiffness matrix. As for the first cantilever example, methods (A) and (B) provide identical results, thus confirming that alternative definitions of rotation can be used without consequential loss in accuracy, and that the simplified rotation matrix of method (A) is accurate within an incremental approach. These results demonstrate further that the accuracy of method (C), whilst independent of the number of incremental steps, can be improved at large displacements through mesh refinement. As shown in Fig. 18, the use of 4 elements per member with method (C) provides an almost identical prediction to that obtained with methods (A) and (B) for the full range of response under consideration.

7 Conclusions

This paper clarifies a number of conceptual issues which are related to the geometrically nonlinear analysis of 3D frames, and which have been a source of previous confusion. The two main issues that are considered are the symmetry of the tangent stiffness matrix and the nature of element end moments.

Following a concise definition of the tangent stiffness matrix, it is shown that symmetry of this matrix can always be achieved for a conservative structural system. This symmetry property is shown to be achieved if the governing equilibrium equations, including those which describe moment equilibrium, are identical to ones derived from a variational energy

approach. Such equations would accordingly be work conjugate with the adopted definition for nodal freedoms, including translations but more significantly rotations. It is also shown that the resulting symmetric tangent stiffness matrix becomes independent of the applied loading if all conservative moment loads, where present, are modelled by means of forces applied at the ends of additional rigid link elements.

The issue concerning the nature of element end moments is then considered, where the inappropriateness of a behavioural linkage between internal (bending and torsional) moments and element nodal moments is highlighted. It is suggested that classification should only be applied to element end moments, and that in fact any related definition can be adopted for the purpose of formulating the response of geometrically nonlinear elements. However, it is proposed that a definition for the nodal moments which implies work conjugacy with the adopted definition for nodal rotations has the benefit of not requiring an a priori classification of these moments. Furthermore, such a definition presents significant computational advantages related to the symmetry of the tangent stiffness matrix and to the assembly of element moment contributions through simple summation. It is also proposed that any definition for nodal rotations which expresses a unique vector transformation can be adopted without compromising modelling accuracy, even though the nature of the work conjugate nodal moments may not be of a standard type. This latter outcome, however, has no practical significance, provided that conservative applied moments are simulated by means of forces acting at the ends of additional rigid link elements.

The previous discussion is illustrated with reference to three variant forms of a large displacement analysis method proposed by the author for 3D frames, each variant method representing a specific instantiation of the variational energy approach. The first, method (A),

employs a definition for incremental nodal rotations which approximates the semi-tangential definition to a second-order, and it employs a local co-rotational system in which the strain-inducing deformations are determined incrementally. The second, method (B), replaces the simplified rotation matrix of method (A) with an exact alternative based on modified Euler angles. Finally, method (C) modifies method (B) through the use of a total instead of an incremental formulation approach.

In all three variant methods, considerable formulation and computational advantages arise from assuming that any applied conservative moments are represented by means of forces acting at the ends of additional rigid link elements. The variant methods lead to alternative, but symmetric, tangent stiffness matrices, and none of these methods requires an a priori classification of the element end moments, although the nature of the work conjugate moments is discussed.

Examples are finally presented to illustrate the accuracy of the three variant methods with reference to several problems of 3D members and frames subject to forces and moments of various types. All examples confirm that alternative definitions of rotation may be used without necessarily compromising solution accuracy, and that the simplified rotation matrix of the original method (A) provides excellent accuracy in the context of an incremental approach. These examples also show that the incremental formulation presents no particular benefits with respect to the main argument of this paper, since very good accuracy is achieved in all cases using the total method (C). Significantly, the last example of a dome structure subject to an apex vertical load shows that the variant methods are all capable of predicting accurately the lowest buckling mode when small imperfections are introduced. Along with the other results, this shows that previously related assertions of an intrinsic asymmetric

characteristic for the tangent stiffness matrix and of a unique prescribed type for the element end moments are in fact misconceptions.

References

[1] C. Oran, *Tangent stiffness in space frames*, J. Struct. Div., ASCE, **99** (1973), 987-1001.

[2] J.H. Argyris, P.C. Dunne, D.W. Scharpf, *On large displacement-small strain analysis of structures with rotational freedoms,* Comp. Meth. Appl. Mech. Engrg., **14** (1978), 401-451; **15** (1978), 99-135.

[3] K. Kondoh, K. Tanaka, S.N. Atluri S.N., *An explicit expression for the tangent-stiffness of a finitely deformed 3-D beam and its use in the analysis of space frames,* Comp. Struct., **24**, (1986), 253-271.

[4] Y.B. Yang, W. McGuire, *Joint rotation and geometric nonlinear analysis*, J. Struct. Engrg., ASCE, **112** (1986), 879-905.

[5] J.L. Meek, S. Loganathan, *Geometrically non-linear behaviour of space frame structures*, Comp. Struct., **31** (1989), 35-45.

[6] K.S. Surana, R.M. Sorem, *Geometrically non-linear formulation for three dimensional curved beam elements with large rotations*, Int. J. Num. Meth. Eng., **28** (1989), 43-73.

[7] Y.B. Yang, S.R. Kuo, *Consistent Frame Buckling Analysis by Finite Element Method*, J. Struct. Engrg., ASCE, **117** (1991), 1053-1069.

[8] B.A. Izzuddin, A.S. Elnashai, *Eulerian formulation for large-displacement analysis of space frames*, J. Engrg. Mech., ASCE, **117** (1993), 549-569.

[9] L.H. Teh, M.J. Clarke, *Symmetry of tangent stiffness matrices of 3D elastic frame*, J. Engrg. Mech., ASCE, **125** (1999), 248-251.

[10] J.F. Besseling, *Derivatives of deformation parameters for bar elements and their use in buckling and postbuckling analysis*, Comp. Meth. Appl. Mech. Engrg., **12** (1977), 97-124.

[11] A. Kassimali, *Large Deformation Analysis of Elastic-Plastic Frames*, J. Struct. Engrg., **109** (1983), 1869-1886.

[12] M.A. Crisfield, *Non-linear finite element analysis of solids and structures*, John Wiley & Sons, Chichester, England, Vol. **1** (1991).

[13] B.A. Izzuddin, D. Lloyd Smith, *Large displacement analysis of elastoplastic thin-walled frames. I: formulation and implementation*, J. Struct. Engrg., ASCE, **122** (1996), 905-914.

[14] B.A. Izzuddin, *Quartic formulation for elastic beam-columns subject to thermal effects*, J. Engrg. Mech., ASCE, **122** (1996), 861-871.

[15] B.A. Izzuddin, *Nonlinear dynamic analysis of framed structures*, PhD thesis, Department of Civil Engineering, Imperial College, University of London, (1991).

[16] B.A. Izzuddin, D. Lloyd Smith, *Large displacement analysis of elastoplastic thin-walled frames. II: verification and application*, J. Struct. Engrg., ASCE, **122** (1996), 915-925.

Appendix A

A.1 Linear local beam-column formulation

With reference to Fig. 2, the linear local response for a beam-column formulation can be derived using the variational energy principle or the virtual work method. This linear response is given by the familiar expression:

$$ {}_{c}\mathbf{f} = {}_{c}\mathbf{k}\ {}_{c}\mathbf{u} \tag{A.1} $$

where ${}_{c}k$ is the constant stiffness matrix, identical in this case to the tangent stiffness matrix, as expressed by:

$$ {}_{c}\mathbf{k} = \frac{1}{L}\begin{bmatrix} 4EI_y & 0 & 2EI_y & 0 & 0 & 0 \\ 0 & 4EI_z & 0 & 2EI_z & 0 & 0 \\ 2EI_y & 0 & 4EI_y & 0 & 0 & 0 \\ 0 & 2EI_z & 0 & 4EI_z & 0 & 0 \\ 0 & 0 & 0 & 0 & EA & 0 \\ 0 & 0 & 0 & 0 & 0 & GJ \end{bmatrix} \tag{A.2} $$

in which EI_y and EI_z are the flexural rigidities in the local x-y and x-z planes, EA is the axial rigidity and GJ is the torsional rigidity.

A.2 Transformation matrix T

The transformation matrix T required in (19) is defined as:

$$ \mathbf{T}_{i,m} = \frac{\partial_{c}\mathbf{u}_{m}}{\partial_{g}\mathbf{u}_{i}} \quad (m = 1 \rightarrow 6\,; \quad i = 1 \rightarrow 12) \tag{A.3} $$

Since the relationship between ${}_{c}\mathbf{u}$ and ${}_{g}\mathbf{u}$ is an implicit one, chain differentiation rules are employed to determine **T** as follows:

$$\mathbf{T}_{i,1} = \frac{\partial \theta_{1y}}{\partial_g \mathbf{u}_i} = \begin{cases} -\sum_{j=1}^{3} \frac{\partial_x \mathbf{c}_j}{\partial_g \mathbf{u}_i} \, {}_{y}^{1}\mathbf{c}_j & (i = 1 \to 3, 7 \to 9) \\ -\sum_{j=1}^{3} {}_{x}\mathbf{c}_j \, \frac{\partial_y^1 \mathbf{c}_j}{\partial_g \mathbf{u}_i} & (i = 4 \to 6) \end{cases} \tag{A.4.a}$$

$$\mathbf{T}_{i,2} = \frac{\partial \theta_{1z}}{\partial_g \mathbf{u}_i} = \begin{cases} -\sum_{j=1}^{3} \frac{\partial_x \mathbf{c}_j}{\partial_g \mathbf{u}_i} \, {}_{z}^{1}\mathbf{c}_j & (i = 1 \to 3, 7 \to 9) \\ -\sum_{j=1}^{3} {}_{x}\mathbf{c}_j \, \frac{\partial_z^1 \mathbf{c}_j}{\partial_g \mathbf{u}_i} & (i = 4 \to 6) \end{cases} \tag{A.4.b}$$

$$\mathbf{T}_{i,3} = \frac{\partial \theta_{2y}}{\partial_g \mathbf{u}_i} = \begin{cases} -\sum_{j=1}^{3} \frac{\partial_x \mathbf{c}_j}{\partial_g \mathbf{u}_i} \, {}_{y}^{2}\mathbf{c}_j & (i = 1 \to 3, 7 \to 9) \\ -\sum_{j=1}^{3} {}_{x}\mathbf{c}_j \, \frac{\partial_y^2 \mathbf{c}_j}{\partial_g \mathbf{u}_i} & (i = 10 \to 12) \end{cases} \tag{A.4.c}$$

$$\mathbf{T}_{i,4} = \frac{\partial \theta_{2z}}{\partial_g \mathbf{u}_i} = \begin{cases} -\sum_{j=1}^{3} \frac{\partial_x \mathbf{c}_j}{\partial_g \mathbf{u}_i} \, {}_{z}^{2}\mathbf{c}_j & (i = 1 \to 3, 7 \to 9) \\ -\sum_{j=1}^{3} {}_{x}\mathbf{c}_j \, \frac{\partial_z^2 \mathbf{c}_j}{\partial_g \mathbf{u}_i} & (i = 10 \to 12) \end{cases} \tag{A.4.d}$$

$$\mathbf{T}_{i,5} = \frac{\partial \Delta}{\partial_g \mathbf{u}_i} = \frac{\partial L_E}{\partial_g \mathbf{u}_i} = \begin{cases} -\,{}_{x}\mathbf{c}_i & (i = 1 \to 3) \\ {}_{x}\mathbf{c}_{i-6} & (i = 7 \to 9) \end{cases} \tag{A.4.e}$$

$$\mathbf{T}_{i,6} = \frac{\partial \theta_T}{\partial_g \mathbf{u}_i} = \begin{cases} \sum_{j=1}^{3} \frac{\partial_z^1 \mathbf{c}_j}{\partial_g \mathbf{u}_i} \, {}_y^{21}\mathbf{c}_j & (i = 4 \to 6) \\ \sum_{j=1}^{3} {}_z^1\mathbf{c}_j \frac{\partial \, {}_y^{21}\mathbf{c}_j}{\partial_g \mathbf{u}_i} & (i = 10 \to 12) \end{cases} \tag{A.4.f}$$

with all remaining terms of **T** being zero.

The first partial derivatives of the cross-sectional orientation vectors, required in (A.4), are given by:

$$\frac{\partial \, {}_x\mathbf{c}_j}{\partial_g \mathbf{u}_i} = \begin{cases} \frac{{}_x\mathbf{c}_i \; {}_x\mathbf{c}_j - \mathbf{I}_{i,j}}{L_E} & (i, j = 1 \to 3) \\ -\frac{\partial \, {}_x\mathbf{c}_j}{\partial_g \mathbf{u}_{i-6}} & (i = 7 \to 9 \,; \quad j = 1 \to 3) \end{cases} \tag{A.5.a}$$

$$\frac{\partial_{y/z}^{n}\mathbf{c}_j}{\partial_g \mathbf{u}_i} = \sum_{k=1}^{3} \frac{\partial \, {}_r^n\mathbf{T}_{j,k}}{\partial_g \mathbf{u}_i} \, {}_{y/z}^{n}\mathbf{c}_k^o \qquad (n = 1 \to 2 \,; \; i = 6n-2 \to 6n \,; \quad j = 1 \to 3) \tag{A.5.b}$$

$$\frac{\partial_y^{21}\mathbf{c}_j}{\partial_g \mathbf{u}_i} = \sum_{k=1}^{3} \frac{\partial \, {}_r^2\mathbf{T}_{j,k}}{\partial_g \mathbf{u}_i} \, {}_y^1\mathbf{c}_k^o \qquad (i = 10 \to 12 \,; \quad j = 1 \to 3) \tag{A.5.c}$$

where, **I** is a 3×3 identity matrix.

For variant method (A), the first partial derivatives of ${}_r\mathbf{T}$, given in (23), are obtained as:

$$\frac{\partial \, {}_r^n\mathbf{T}}{\partial \alpha_n} = \begin{bmatrix} 0 & \frac{\beta_n}{2} & \frac{\gamma_n}{2} \\ \frac{\beta_n}{2} & -\alpha_n & -1 \\ \frac{\gamma_n}{2} & 1 & -\alpha_n \end{bmatrix} \qquad (n = 1 \to 2) \tag{A.6.a}$$

$$\frac{\partial\ {}^{n}_{r}\mathbf{T}}{\partial\beta_n}=\begin{bmatrix}-\beta_n & \frac{\alpha_n}{2} & 1\\ \frac{\alpha_n}{2} & 0 & \frac{\gamma_n}{2}\\ -1 & \frac{\gamma_n}{2} & -\beta_n\end{bmatrix}\qquad (n=1\rightarrow 2) \tag{A.6.b}$$

$$\frac{\partial\ {}^{n}_{r}\mathbf{T}}{\partial\gamma_n}=\begin{bmatrix}-\gamma_n & -1 & \frac{\alpha_n}{2}\\ 1 & -\gamma_n & \frac{\beta_n}{2}\\ \frac{\alpha_n}{2} & \frac{\beta_n}{2} & 0\end{bmatrix}\qquad (n=1\rightarrow 2) \tag{A.6.c}$$

For variant methods (B) and (C), only (A.6) is modified, where the first partial derivatives of ${}_{r}\mathbf{T}$ with respect to the global rotational freedoms are derived from (26).

A.3 Array g

The three dimensional array **g** required in (20) for determining the geometric stiffness matrix is defined as:

$$\mathbf{g}_{i,j,m}=\frac{\partial^2\ {}_{c}\mathbf{u}_m}{\partial_g\mathbf{u}_i\,\partial_g\mathbf{u}_j}\qquad (i,j=1\rightarrow 12\ ;\quad m=1\rightarrow 6) \tag{A.7}$$

The individual terms of **g** are obtained using chain differentiation rules as follows:

$$\mathbf{g}_{i,j,1}=\frac{\partial^2\theta_{1y}}{\partial_g\mathbf{u}_i\,\partial_g\mathbf{u}_j}=\begin{cases}-\sum_{k=1}^{3}\dfrac{\partial^2\ {}_{x}\mathbf{c}_k}{\partial_g\mathbf{u}_i\,\partial_g\mathbf{u}_j}\ {}^{1}_{y}\mathbf{c}_k & (i,j=1\rightarrow 3,7\rightarrow 9)\\ -\sum_{k=1}^{3}\dfrac{\partial_x\mathbf{c}_k}{\partial_g\mathbf{u}_i}\dfrac{\partial\ {}^{1}_{y}\mathbf{c}_k}{\partial_g\mathbf{u}_j} & (i=1\rightarrow 3,7\rightarrow 9\ ;\ \ j=4\rightarrow 6)\\ -\sum_{k=1}^{3}{}_{x}\mathbf{c}_k\dfrac{\partial^2\ {}^{1}_{y}\mathbf{c}_k}{\partial_g\mathbf{u}_i\,\partial_g\mathbf{u}_j} & (i,j=4\rightarrow 6)\end{cases} \tag{A.8.a}$$

$$\mathbf{g}_{i,j,2} = \frac{\partial^2 \theta_{1z}}{\partial_g \mathbf{u}_i \, \partial_g \mathbf{u}_j} = \begin{cases} -\sum_{k=1}^{3} \frac{\partial^2 {}_x\mathbf{c}_k}{\partial_g \mathbf{u}_i \, \partial_g \mathbf{u}_j} \; {}^1_z\mathbf{c}_k & (i, j = 1 \to 3, 7 \to 9) \\ -\sum_{k=1}^{3} \frac{\partial_x \mathbf{c}_k}{\partial_g \mathbf{u}_i} \frac{\partial \, {}^1_z\mathbf{c}_k}{\partial_g \mathbf{u}_j} & (i = 1 \to 3, 7 \to 9 \,;\; j = 4 \to 6) \\ -\sum_{k=1}^{3} {}_x\mathbf{c}_k \; \frac{\partial^2 \, {}^1_z\mathbf{c}_k}{\partial_g \mathbf{u}_i \, \partial_g \mathbf{u}_j} & (i, j = 4 \to 6) \end{cases} \quad \text{(A.8.b)}$$

$$\mathbf{g}_{i,j,3} = \frac{\partial^2 \theta_{2y}}{\partial_g \mathbf{u}_i \, \partial_g \mathbf{u}_j} = \begin{cases} -\sum_{k=1}^{3} \frac{\partial^2 {}_x\mathbf{c}_k}{\partial_g \mathbf{u}_i \, \partial_g \mathbf{u}_j} \; {}^2_y\mathbf{c}_k & (i, j = 1 \to 3, 7 \to 9) \\ -\sum_{k=1}^{3} \frac{\partial_x \mathbf{c}_k}{\partial_g \mathbf{u}_i} \frac{\partial \, {}^2_y\mathbf{c}_k}{\partial_g \mathbf{u}_j} & (i = 1 \to 3, 7 \to 9 \,;\; j = 10 \to 12) \\ -\sum_{k=1}^{3} {}_x\mathbf{c}_k \; \frac{\partial^2 \, {}^2_y\mathbf{c}_k}{\partial_g \mathbf{u}_i \, \partial_g \mathbf{u}_j} & (i, j = 10 \to 12) \end{cases} \quad \text{(A.8.c)}$$

$$\mathbf{g}_{i,j,4} = \frac{\partial^2 \theta_{2z}}{\partial_g \mathbf{u}_i \, \partial_g \mathbf{u}_j} = \begin{cases} -\sum_{k=1}^{3} \frac{\partial^2 {}_x\mathbf{c}_k}{\partial_g \mathbf{u}_i \, \partial_g \mathbf{u}_j} \; {}^2_z\mathbf{c}_k & (i, j = 1 \to 3, 7 \to 9) \\ -\sum_{k=1}^{3} \frac{\partial_x \mathbf{c}_k}{\partial_g \mathbf{u}_i} \frac{\partial \, {}^2_z\mathbf{c}_k}{\partial_g \mathbf{u}_j} & (i = 1 \to 3, 7 \to 9 \,;\; j = 10 \to 12) \\ -\sum_{k=1}^{3} {}_x\mathbf{c}_k \; \frac{\partial^2 \, {}^2_z\mathbf{c}_k}{\partial_g \mathbf{u}_i \, \partial_g \mathbf{u}_j} & (i, j = 10 \to 12) \end{cases} \quad \text{(A.8.d)}$$

$$\mathbf{g}_{i,j,5} = \frac{\partial^2 \Delta}{\partial_g \mathbf{u}_i \, \partial_g \mathbf{u}_j} = \frac{\partial^2 L_E}{\partial_g \mathbf{u}_i \, \partial_g \mathbf{u}_j} = \begin{cases} -\frac{\partial_x \mathbf{c}_j}{\partial_g \mathbf{u}_i} & (i = 1 \to 3, 7 \to 9 \,;\; j = 1 \to 3) \\ -\frac{\partial_x \mathbf{c}_{j-6}}{\partial_g \mathbf{u}_i} & (i = 1 \to 3, 7 \to 9 \,;\; j = 7 \to 9) \end{cases} \quad \text{(A.8.e)}$$

$$\mathbf{g}_{i,j,6} = \frac{\partial^2 \theta_T}{\partial_g \mathbf{u}_i \, \partial_g \mathbf{u}_j} = \begin{cases} \sum_{k=1}^{3} \frac{\partial^2 \, {}^{1}_{z}\mathbf{c}_k}{\partial_g \mathbf{u}_i \, \partial_g \mathbf{u}_j} \, {}^{21}_{y}\mathbf{c}_k & (i, j = 4 \to 6) \\ \sum_{k=1}^{3} \frac{\partial \, {}^{1}_{z}\mathbf{c}_k}{\partial_g \mathbf{u}_i} \frac{\partial \, {}^{21}_{y}\mathbf{c}_k}{\partial_g \mathbf{u}_j} & (i = 4 \to 6 \,;\; j = 10 \to 12) \\ \sum_{k=1}^{3} {}^{1}_{z}\mathbf{c}_k \frac{\partial^2 \, {}^{21}_{y}\mathbf{c}_k}{\partial_g \mathbf{u}_i \, \partial_g \mathbf{u}_j} & (i, j = 10 \to 12) \end{cases} \qquad \text{(A.8.f)}$$

$$\mathbf{g}_{j,i,m} = \mathbf{g}_{i,j,m} \quad (i = 1 \to 12 \,;\quad j = i+1 \to 12 \,;\quad m = 1 \to 6) \qquad \text{(A.8.g)}$$

with all remaining terms of **g** being zero.

The first partial derivatives of the cross-sectional orientation vectors are given in Appendix A.2, whilst the second partial derivatives are obtained as:

$$\frac{\partial^2 \, {}_{x}\mathbf{c}_k}{\partial_g \mathbf{u}_i \, \partial_g \mathbf{u}_j} = \begin{cases} \frac{3 \, {}_{x}\mathbf{c}_i \, {}_{x}\mathbf{c}_j \, {}_{x}\mathbf{c}_k - {}_{x}\mathbf{c}_i \, \mathbf{I}_{j,k} - {}_{x}\mathbf{c}_j \, \mathbf{I}_{i,k} - {}_{x}\mathbf{c}_k \, \mathbf{I}_{i,j}}{L_E^2} & (i, j, k = 1 \to 3) \\ -\frac{\partial^2 \, {}_{x}\mathbf{c}_k}{\partial_g \mathbf{u}_i \, \partial_g \mathbf{u}_{j-6}} & (i, k = 1 \to 3 \,;\; j = 7 \to 9) \\ \frac{\partial^2 \, {}_{x}\mathbf{c}_k}{\partial_g \mathbf{u}_{i-6} \, \partial_g \mathbf{u}_{j-6}} & (i, j = 7 \to 9 \,;\quad k = 1 \to 3) \end{cases} \qquad \text{(A.9.a)}$$

$$\frac{\partial^2 \, {}^{n}_{y/z}\mathbf{c}_k}{\partial_g \mathbf{u}_i \, \partial_g \mathbf{u}_j} = \sum_{p=1}^{3} \frac{\partial^2 \, {}^{n}_{r}\mathbf{T}_{k,p}}{\partial_g \mathbf{u}_i \, \partial_g \mathbf{u}_j} \, {}^{n}_{y/z}\mathbf{c}^{o}_{p} \quad (n = 1 \to 2 \,;\; i, j = 6n-2 \to 6n \,;\; k = 1 \to 3) \qquad \text{(A.9.b)}$$

$$\frac{\partial^2 \, {}^{21}_{y}\mathbf{c}_k}{\partial_g \mathbf{u}_i \, \partial_g \mathbf{u}_j} = \sum_{p=1}^{3} \frac{\partial^2 \, {}^{2}_{r}\mathbf{T}_{k,p}}{\partial_g \mathbf{u}_i \, \partial_g \mathbf{u}_j} \, {}^{1}_{y}\mathbf{c}^{o}_{p} \quad (i, j = 10 \to 12 \,;\quad k = 1 \to 3) \qquad \text{(A.9.c)}$$

where, **I** is a 3×3 identity matrix, and for variant method (A):

$$\frac{\partial^2 {}^{n}_{r}\mathbf{T}}{\partial \alpha_n^2} = \begin{bmatrix} 0 & 0 & 0 \\ 0 & -1 & 0 \\ 0 & 0 & -1 \end{bmatrix} \quad (n = 1 \rightarrow 2) \tag{A.10.a}$$

$$\frac{\partial^2 {}^{n}_{r}\mathbf{T}}{\partial \alpha_n \, \partial \beta_n} = \frac{\partial^2 {}^{n}_{r}\mathbf{T}}{\partial \beta_n \, \partial \alpha_n} = \begin{bmatrix} 0 & 1/2 & 0 \\ 1/2 & 0 & 0 \\ 0 & 0 & 0 \end{bmatrix} \quad (n = 1 \rightarrow 2) \tag{A.10.b}$$

$$\frac{\partial^2 {}^{n}_{r}\mathbf{T}}{\partial \alpha_n \, \partial \gamma_n} = \frac{\partial^2 {}^{n}_{r}\mathbf{T}}{\partial \gamma_n \, \partial \alpha_n} = \begin{bmatrix} 0 & 0 & 1/2 \\ 0 & 0 & 0 \\ 1/2 & 0 & 0 \end{bmatrix} \quad (n = 1 \rightarrow 2) \tag{A.10.c}$$

$$\frac{\partial^2 {}^{n}_{r}\mathbf{T}}{\partial \beta_n^2} = \begin{bmatrix} -1 & 0 & 0 \\ 0 & 0 & 0 \\ 0 & 0 & -1 \end{bmatrix} \quad (n = 1 \rightarrow 2) \tag{A.10.d}$$

$$\frac{\partial^2 {}^{n}_{r}\mathbf{T}}{\partial \beta_n \, \partial \gamma_n} = \frac{\partial^2 {}^{n}_{r}\mathbf{T}}{\partial \gamma_n \, \partial \beta_n} = \begin{bmatrix} 0 & 0 & 0 \\ 0 & 0 & 1/2 \\ 0 & 1/2 & 0 \end{bmatrix} \quad (n = 1 \rightarrow 2) \tag{A.10.e}$$

$$\frac{\partial^2 {}^{n}_{r}\mathbf{T}}{\partial \gamma_n^2} = \begin{bmatrix} -1 & 0 & 0 \\ 0 & -1 & 0 \\ 0 & 0 & 0 \end{bmatrix} \quad (n = 1 \rightarrow 2) \tag{A.10.f}$$

For variant methods (B) and (C), only (A.6) and (A.10) are modified to include the first and second partial derivatives of ${}_{r}\mathbf{T}$ with respect to the global rotational freedoms, as can be readily determined from (26).

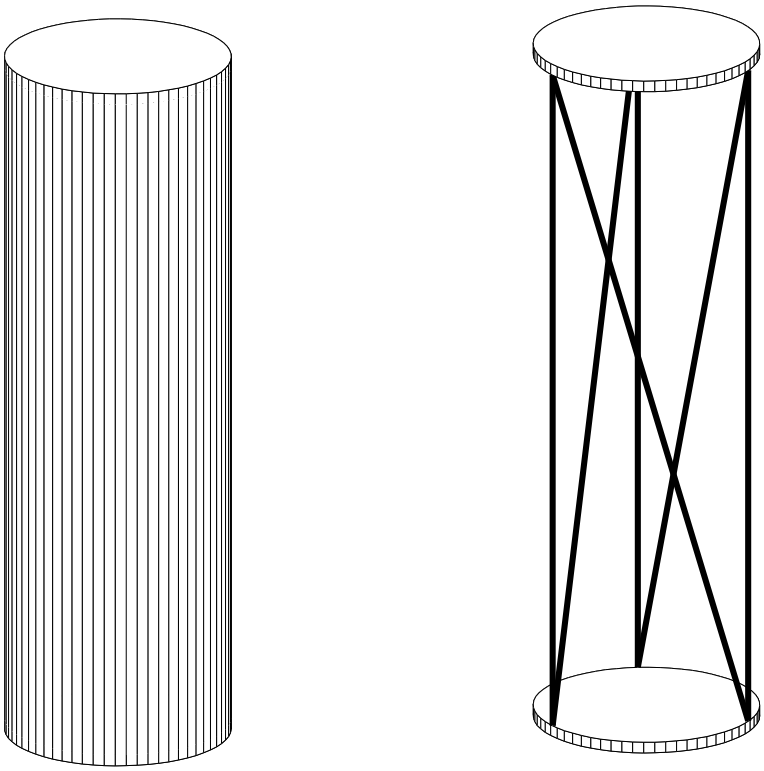

Figure 1. Two beam-column elements with identical nodal interface

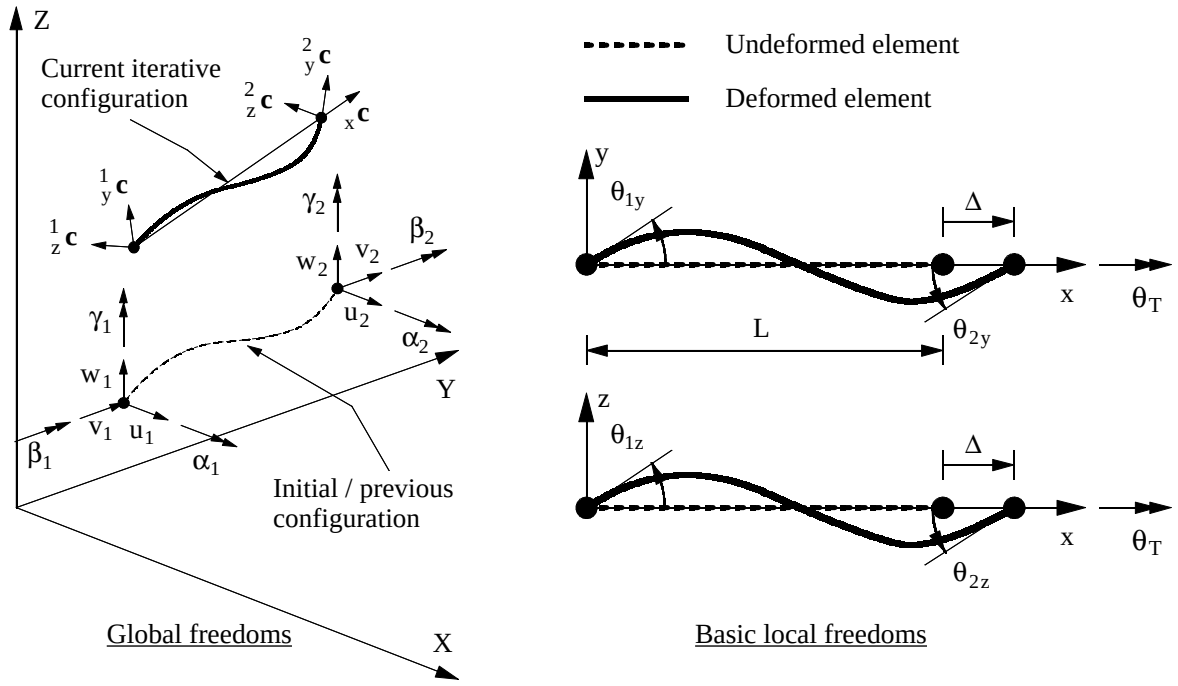

Figure 2. Global and local element freedoms

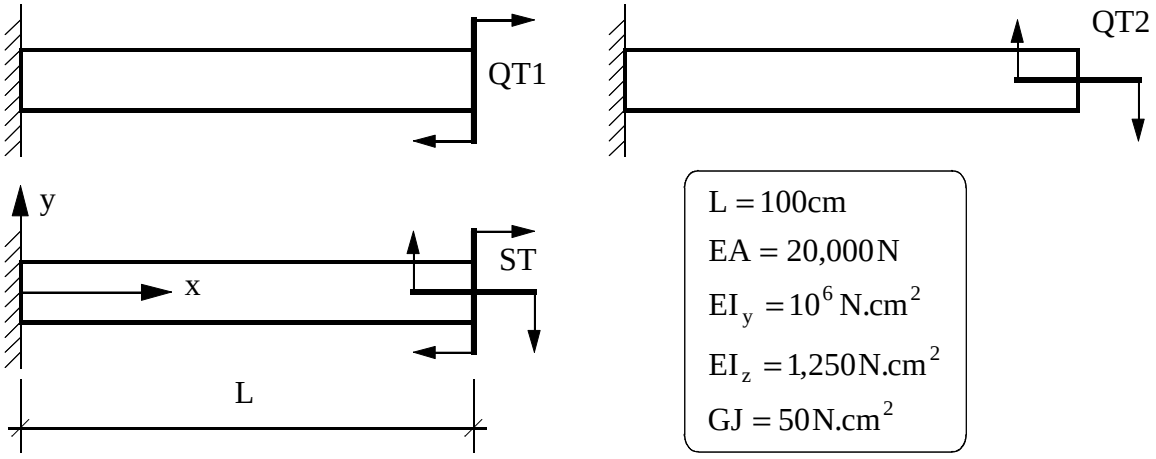

Figure 3. Cantilever subject to quasi- and semi-tangential moments

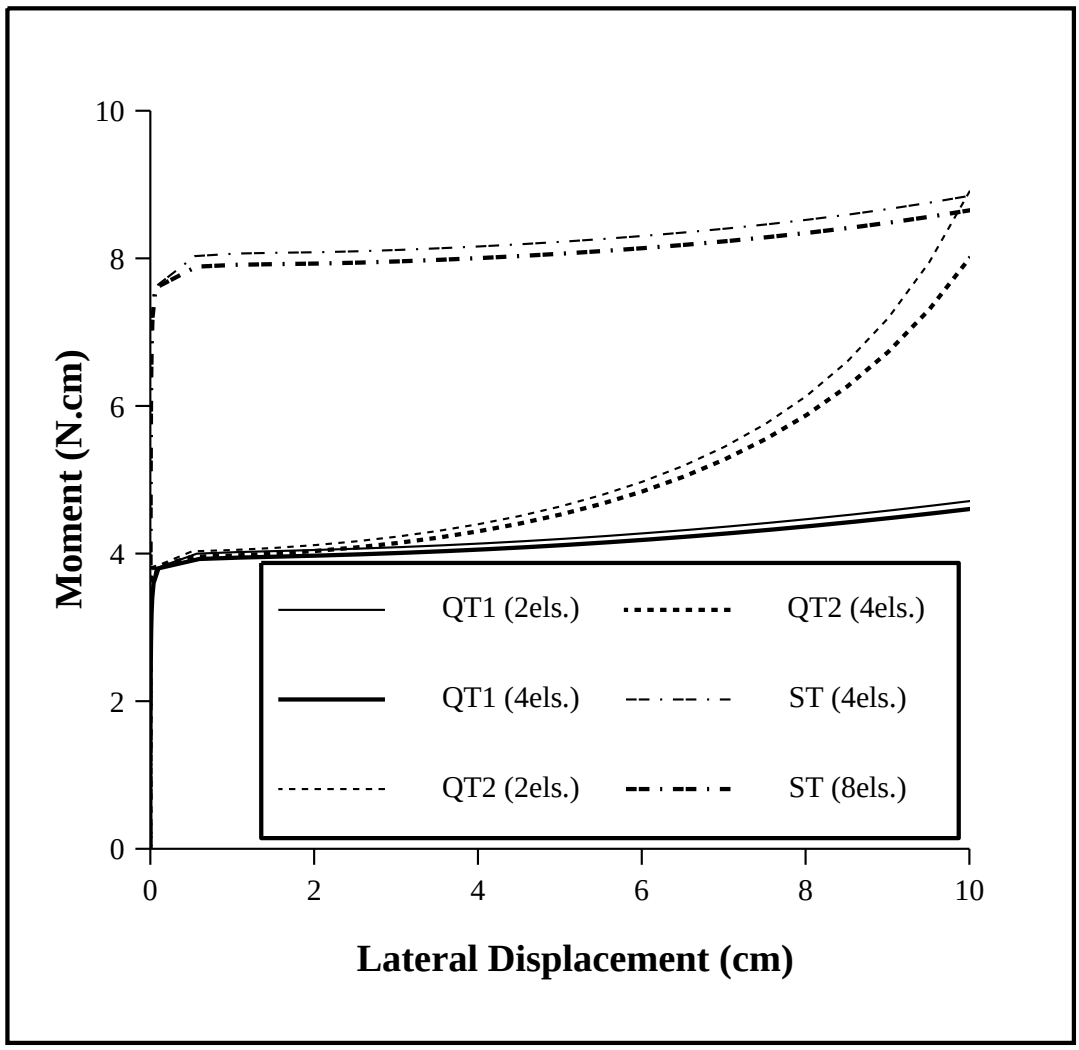

Figure 4. Nonlinear response of cantilever subject to end moment: Method (A)

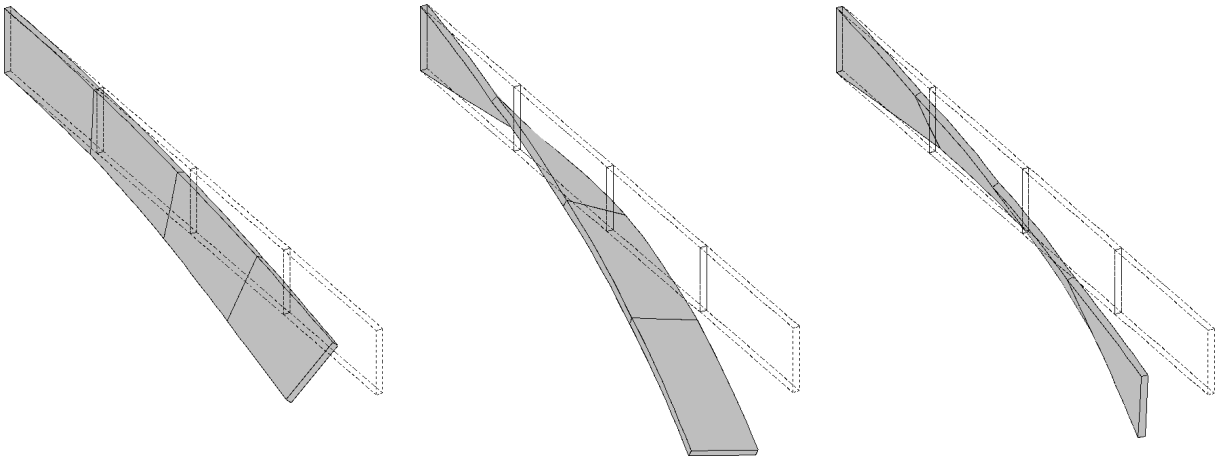

Moment: QT1 **Moment: QT2** **Moment: ST**

Figure 5. Final deflected shapes of cantilever subject to end moment

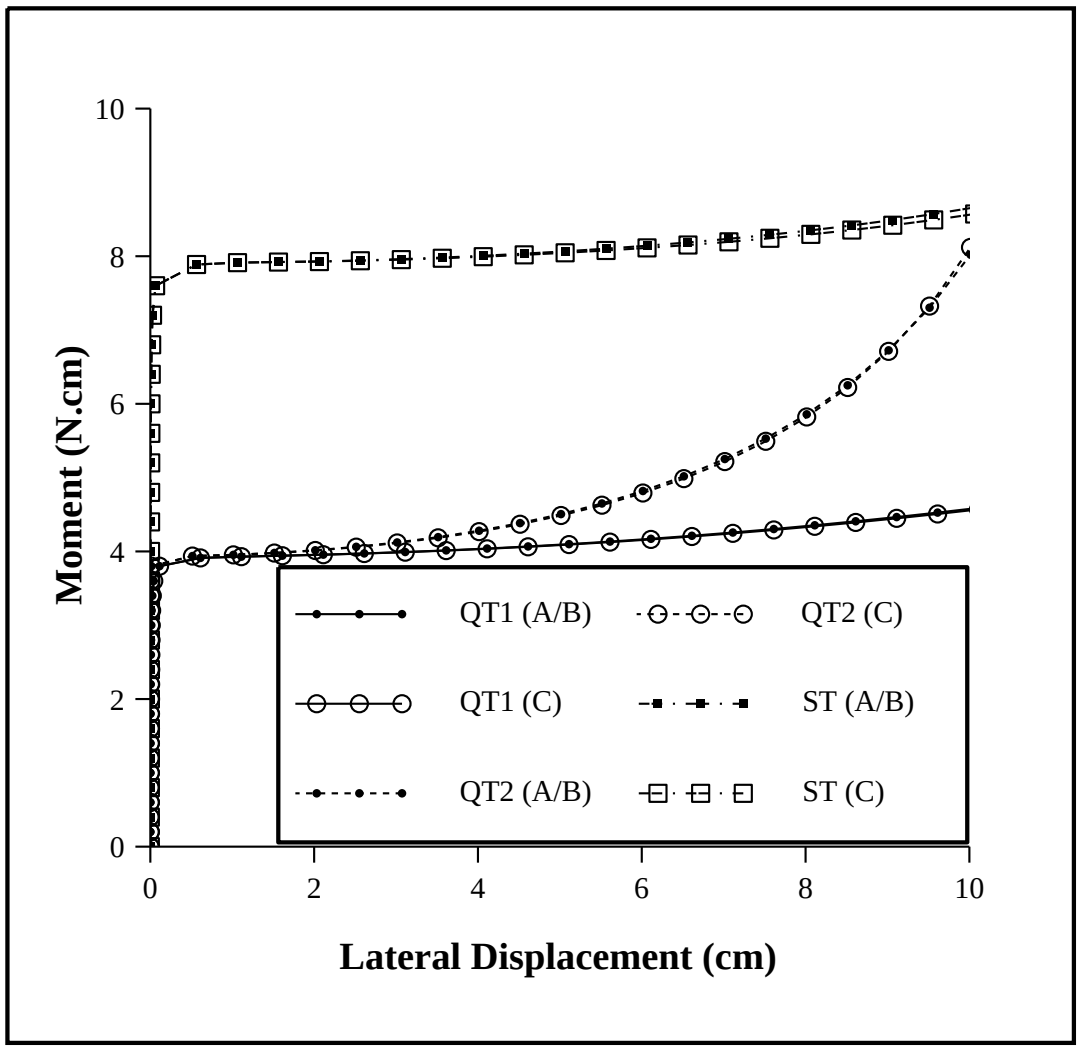

Figure 6. Response of cantilever using variant methods (A) to (C)

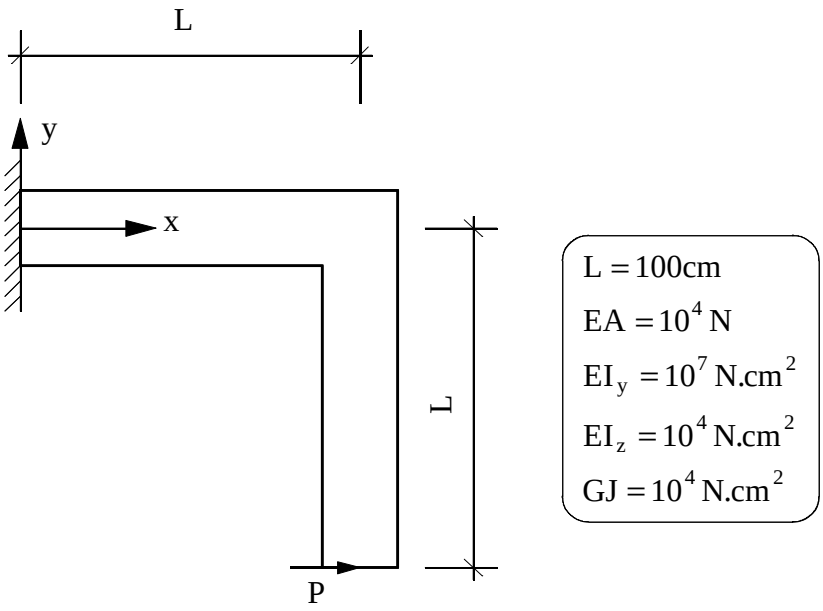

Figure 7. Configuration of L-frame subject to end force

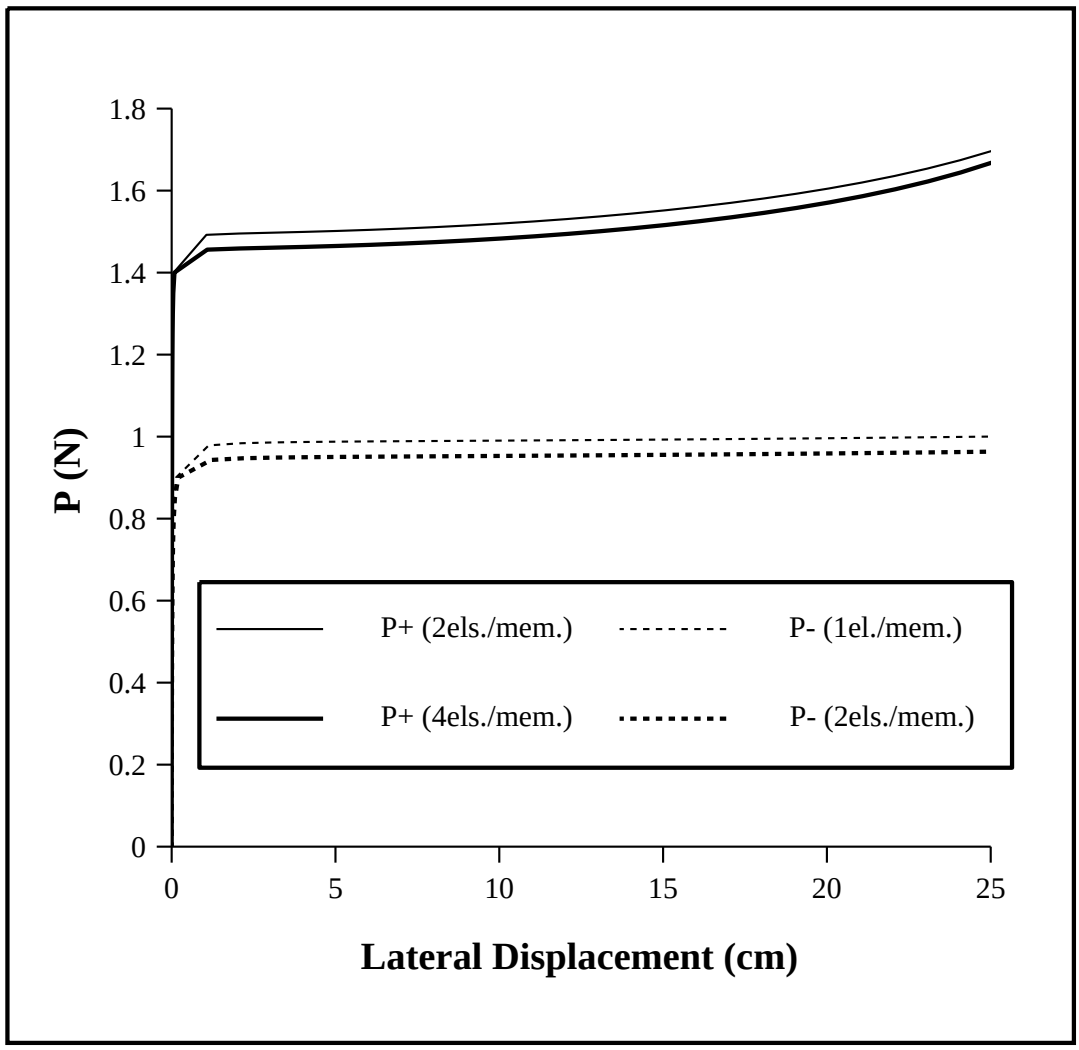

Figure 8. Response of L-frame subject to end force: Method (A)

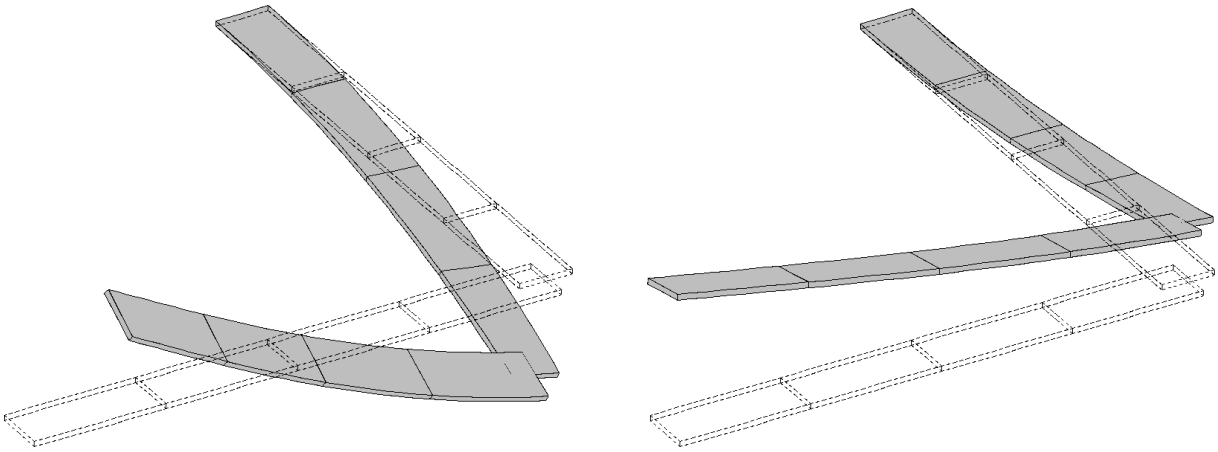

Force: P+ **Force: P-**

Figure 9. Final deflected shapes of L-frame subject to end force

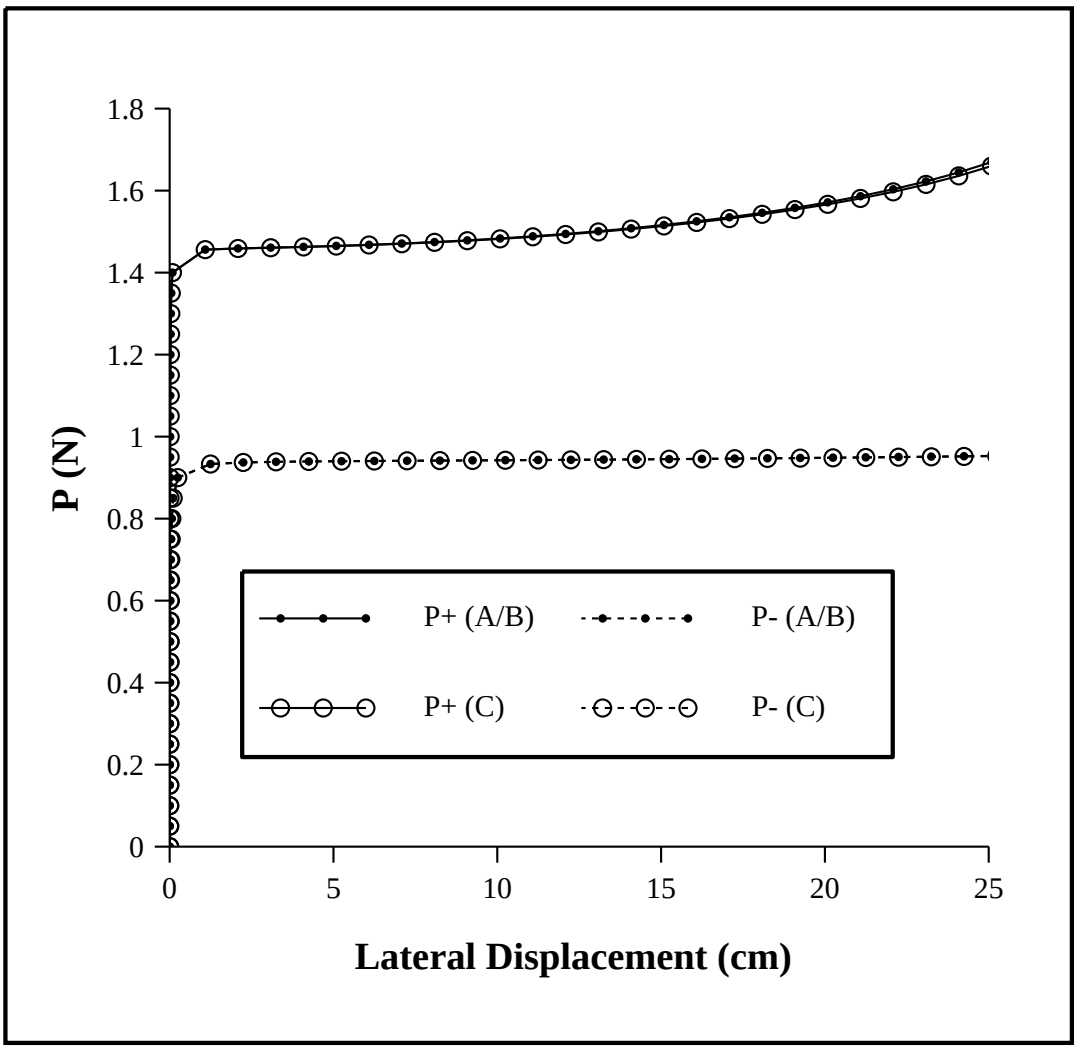

Figure 10. Response of L-Frame subject to end force using variant methods (A) to (C)

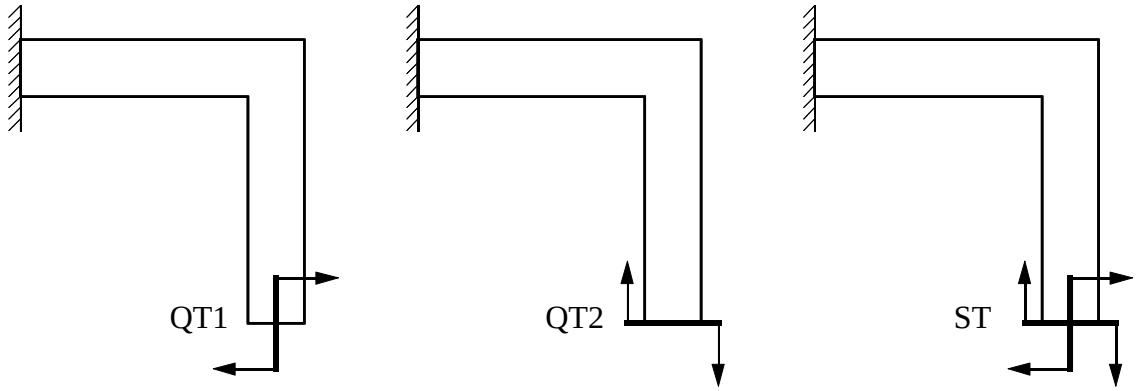

Figure 11. Configuration of L-frame subject to end moments

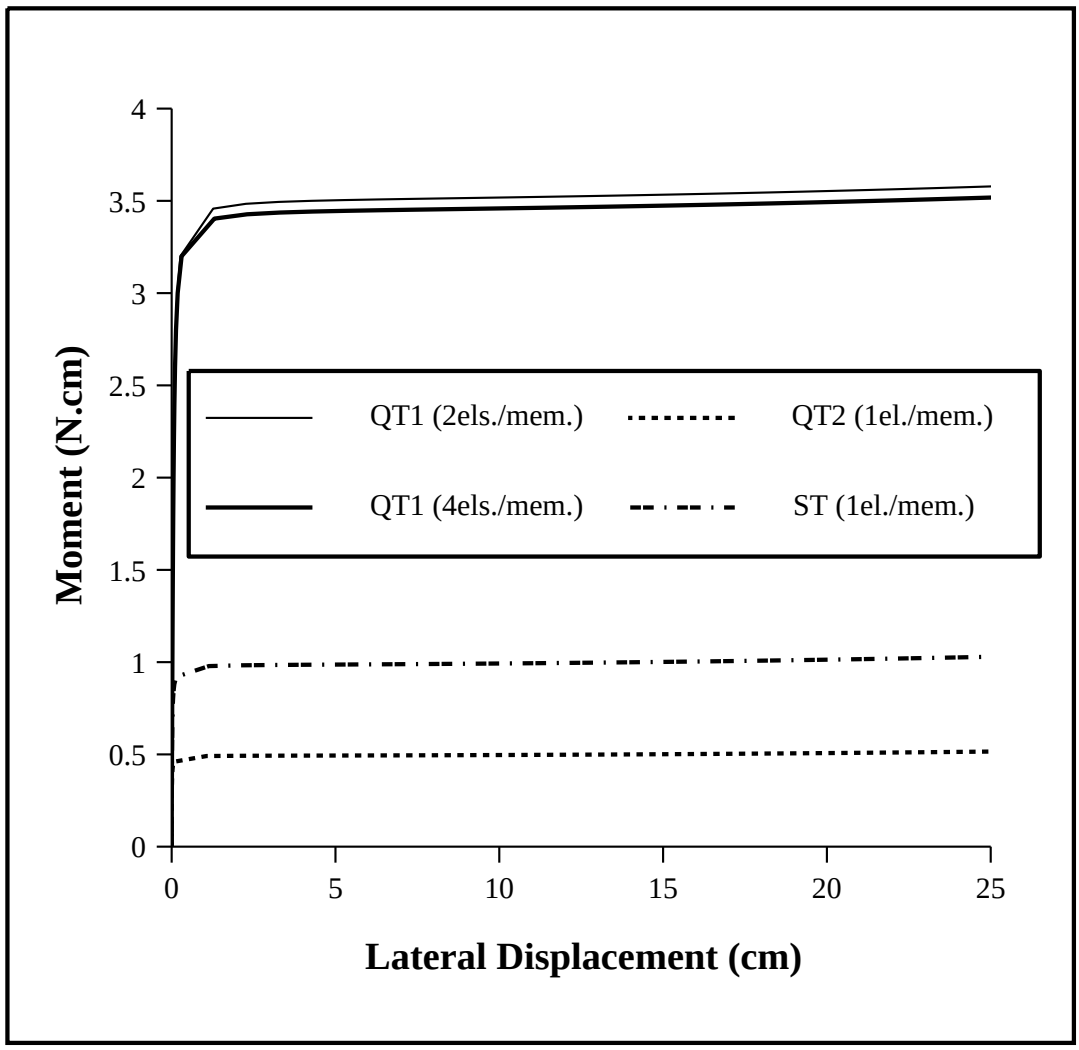

Figure 12. Response of L-frame subject to end moment: Method (A)

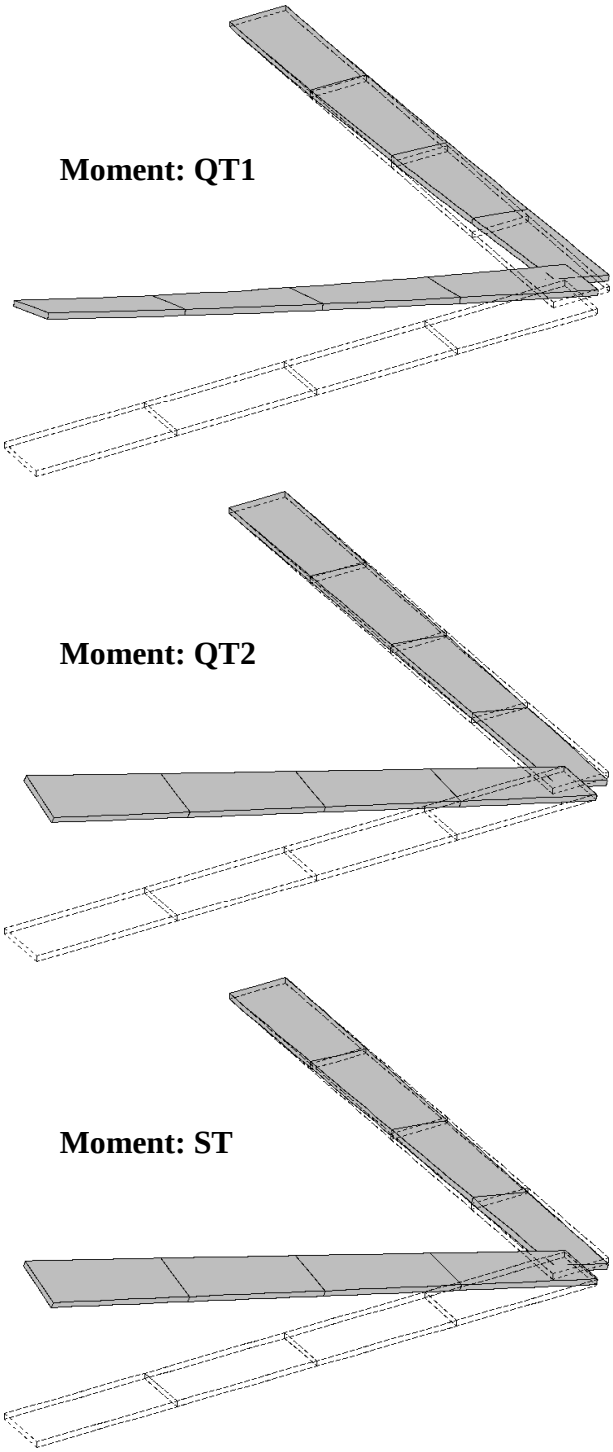

Figure 13. Final deflected shapes of L-frame subject to end moment

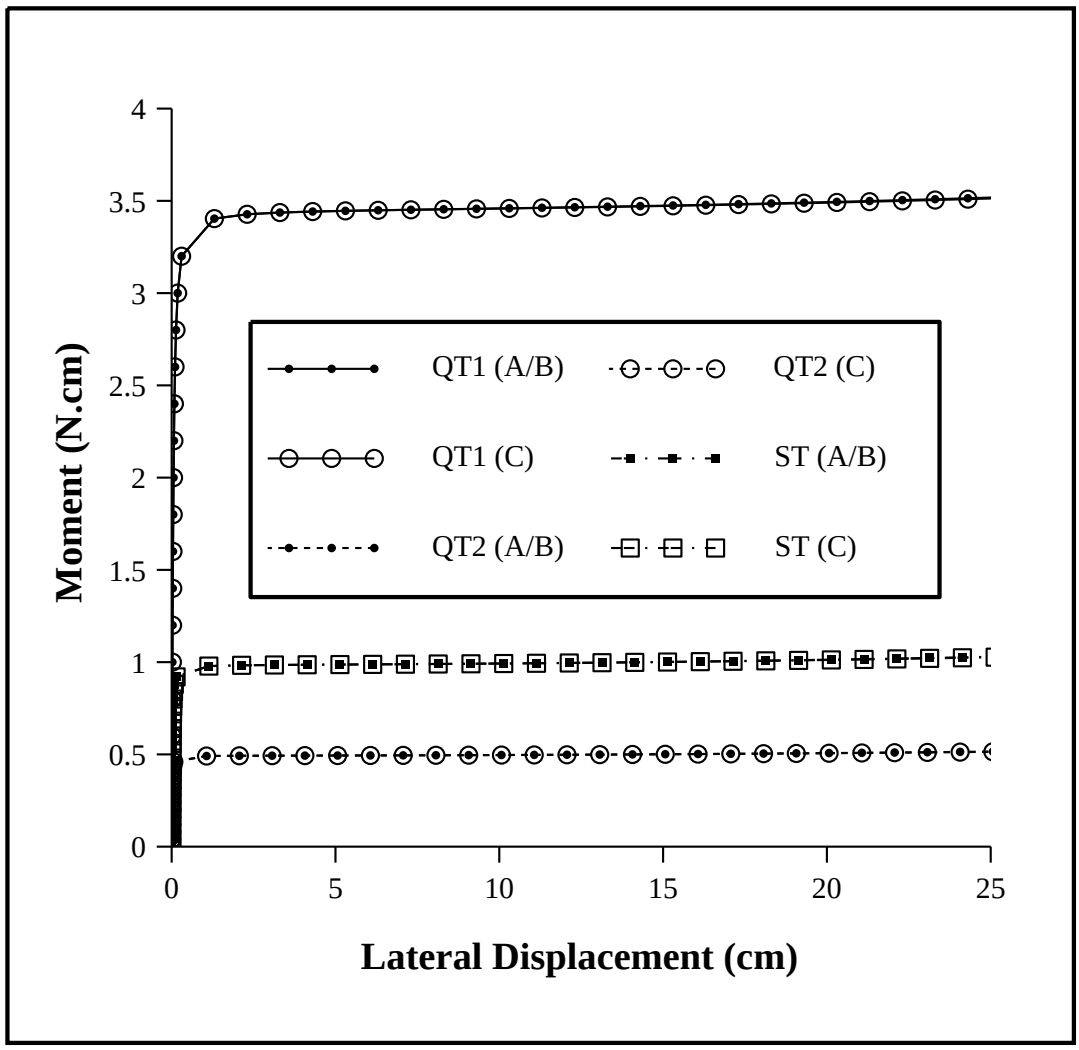

Figure 14. Response of L-Frame subject to end moment using variant methods (A) to (C)

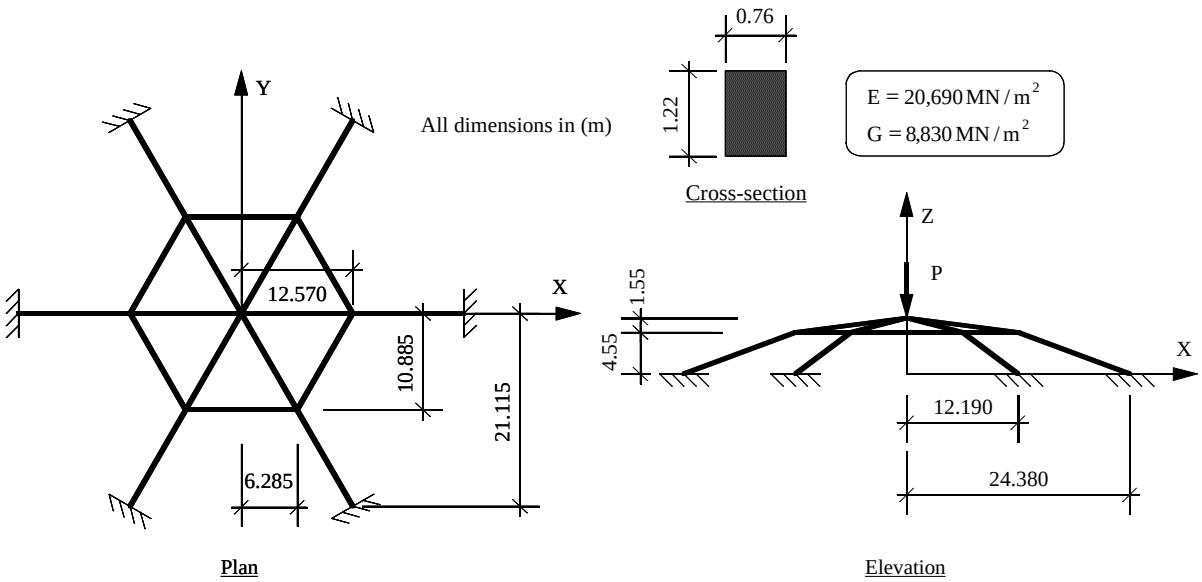

Figure 15. Configuration of space dome subject to a vertical apex load

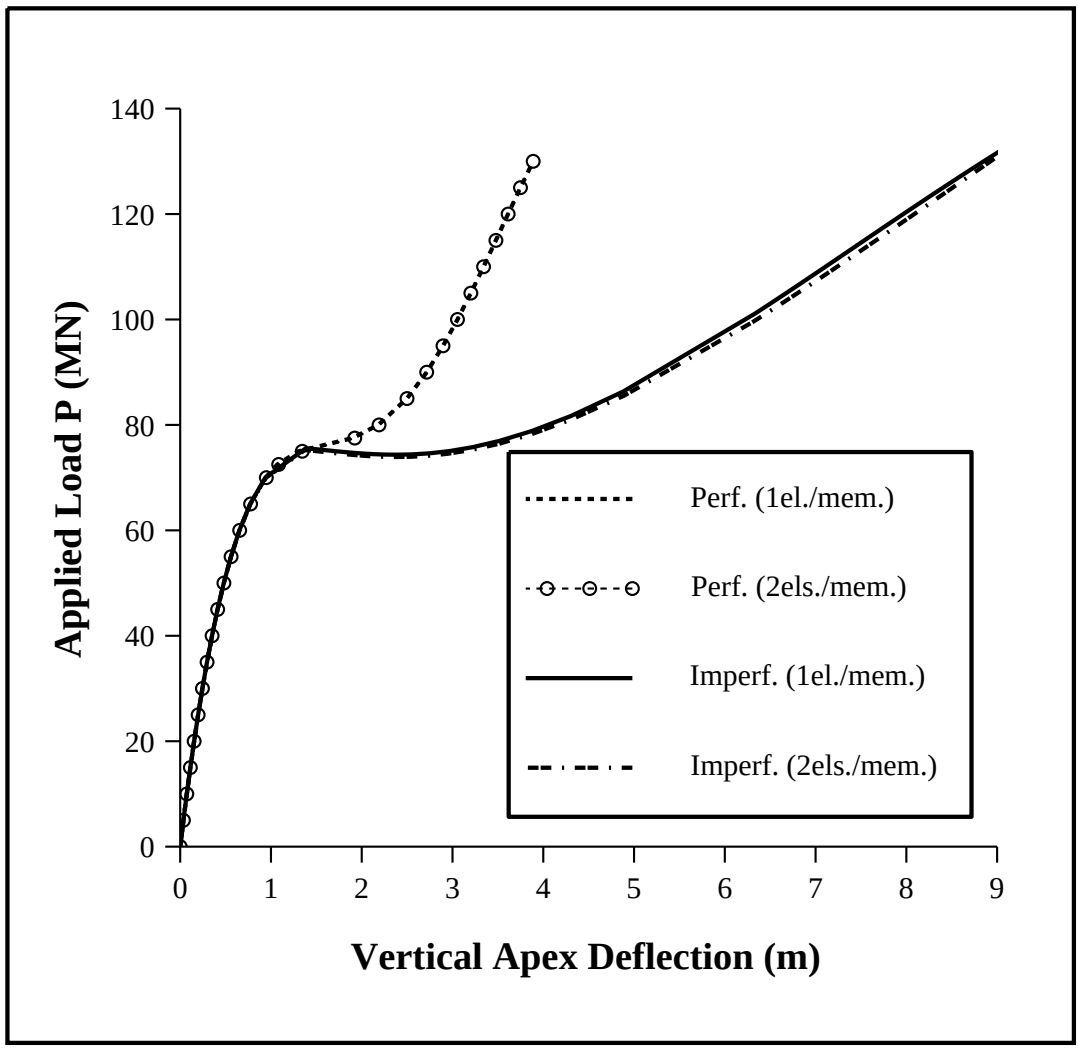

Figure 16. Response of space dome structure: Method (A)

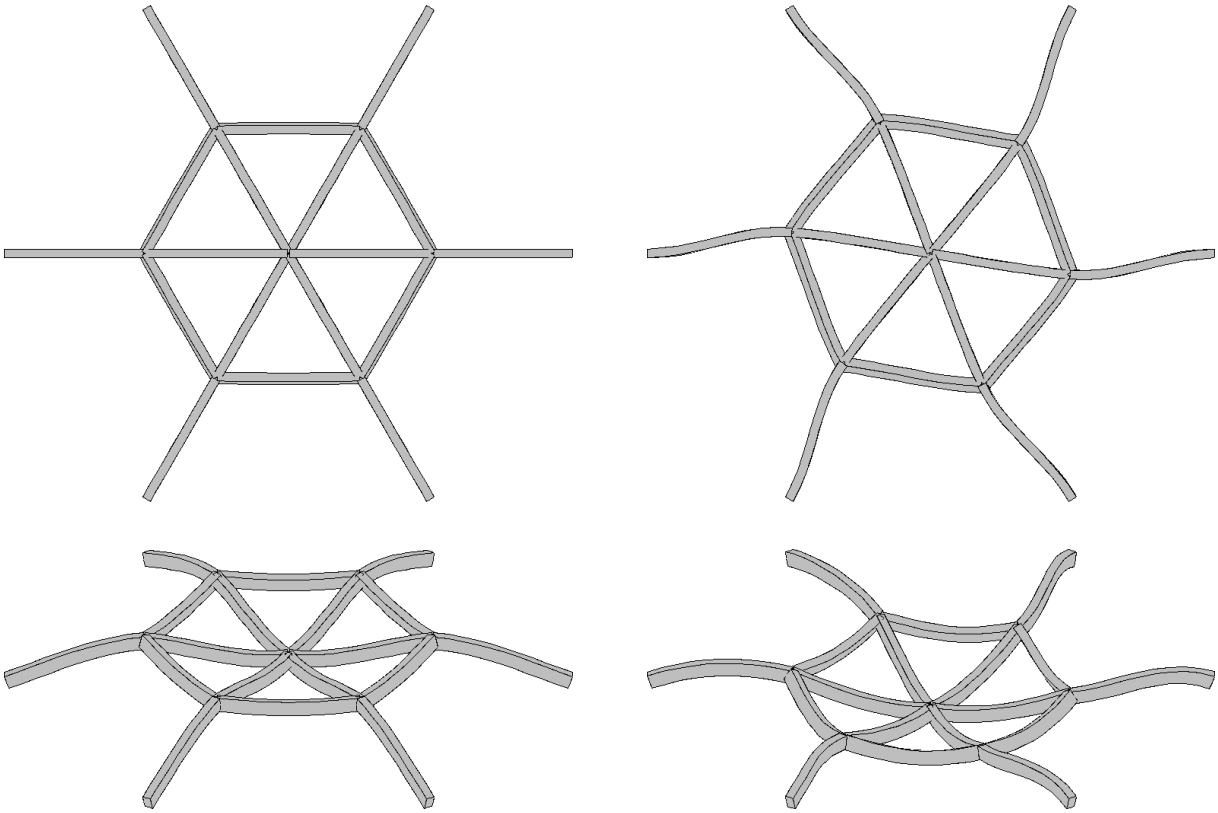

Perfect dome **Imperfect dome**

Figure 17. Final deflected shapes of space dome

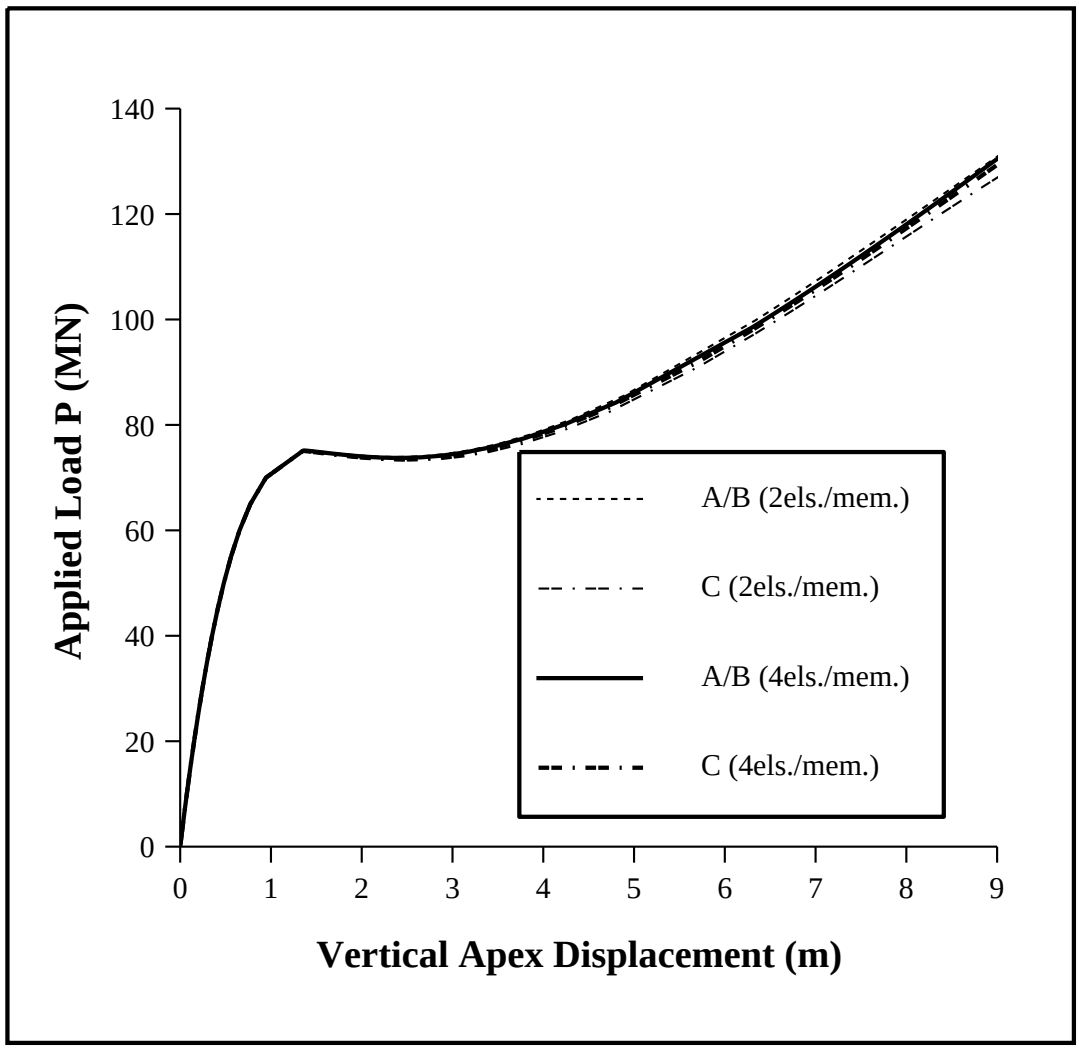

Figure 18. Response of imperfect space dome using variant methods (A) to (C)